UNIVERSITÀ
DEGLI STUDI
DI PADOVA

DIPARTIMENTO
DI INGEGNERIA
DELL'INFORMAZIONE

DIPARTIMENTO DI INGEGNERIA DELL'INFORMAZIONE

CORSO DI LAUREA MAGISTRALE IN BIOINGEGNERIA

Postural control in upper limb functional tasks during standing

Relatrice: Maria Rubega, PhD

Laureanda: Alessia Nepitali

Correlatrici: Paola Contessa, PhD
Dott.ssa Erika Venturini

ANNO ACCADEMICO 2023 – 2024

Data di laurea 5 Marzo 2024

ABSTRACT

This thesis is based on a project aimed at validating an innovative therapy for the treatment of upper limb lymphedema. Lymphedema is a debilitating disease with a slow and progressive course that may result in a loss of quality of life if appropriate therapy is not initiated early. Breast cancer is the most common cause of upper limb lymphedema. Increased arm volume can lead to gait and balance problems as a result of changes in postural control strategies.

The objective of this thesis is to study postural control in upper limb functional tasks during standing by analyzing the Center of Pressure (CoP) signal. A group of 11 healthy women and 2 patients with lymphedema participated in this study and were asked to perform a series of tasks in an environment equipped with an optoelectronic system and a force platform. We analyzed balance maintenance during bilateral stance with open-eyes and closed-eyes, unilateral stance and several upper limb functional tasks. Since several repetitions were performed for each task, an algorithm was developed to analyze the movement of the markers placed on the participant's body in order to identify the start and end moments of the movement. In this way, the intervals of interest for the CoP analysis were found. The main parameters extracted from the CoP signal are the position parameters such as the oscillation ranges in the medio-lateral and antero-posterior direction, the confidence ellipse at 95%, the shift of the mean CoP with respect to an axis of symmetry and the dynamic parameters such as the sway path and the sway area. Some exercises proved to be more effective in evaluating a different postural control strategy between control group and patients with lymphedema: unilateral stance, frontal reaching and lateral reaching. In addition, the sway path parameter proved to be the most effective in discriminating between performing the exercise with eyes open and eyes closed. For lymphedema patients, worsening of proprioception may be a possible consequence of cancer treatment, so the proposed analysis may be useful in evaluating the effects of the therapy. In the future, a larger sample size is needed to validate our conclusions.

Regarding the structure of this thesis, Chapter 1 explains in detail what lymphedema is and what treatments are conventionally performed. Furthermore, the methods reported in the literature to evaluate postural control starting from the CoP signal are presented. Subsequently, Chapter 2 describes the participants, the equipment used, the protocol to acquire the signals of

interest and the data analysis algorithm. The latter is divided into two parts, analyzing the data coming from the optoelectronic system and the force platform, respectively. Chapter 3 reports the results obtained, Chapter 4 gives a discussion, and, finally, Chapter 5 summarizes the conclusions of this study.

SOMMARIO

Questa tesi si basa su un progetto volto a validare una terapia innovativa per il trattamento del linfedema agli arti superiori. Il linfedema è una malattia debilitante con un decorso lento e progressivo che può provocare una perdita di qualità della vita se la terapia appropriata non viene iniziata presto. Il cancro al seno è la causa più comune di linfedema agli arti superiori. L'aumento del volume del braccio può portare a problemi di andatura e di equilibrio a causa di cambiamenti nelle strategie di controllo posturale.

L'obiettivo di questa tesi è quello di studiare il controllo posturale durante esercizi funzionali con gli arti superiori in posizione eretta analizzando il segnale del Centro di Pressione (CoP). Un gruppo di 11 donne sane e 2 pazienti con linfedema hanno partecipato a questo studio e gli è stato chiesto di svolgere una serie di esercizi in un ambiente dotato di un sistema optoelettronico e una piattaforma di forza. Abbiamo analizzato il mantenimento dell'equilibrio durante l'appoggio bilaterale con occhi aperti e occhi chiusi, l'appoggio unilaterale e diversi esercizi funzionali con gli arti superiori. Poiché per ogni esercizio sono state eseguite diverse ripetizioni, è stato sviluppato un algoritmo per analizzare il movimento dei marcatori posizionati sul corpo del partecipante al fine di identificare gli istanti iniziali e finali del movimento. In questo modo sono stati individuati gli intervalli di interesse per l'analisi del CoP. I principali parametri estratti dal segnale del CoP sono i parametri di posizione come gli intervalli di oscillazione nella direzione medio-laterale e antero-posteriore, l'ellisse di confidenza al 95%, lo spostamento del CoP medio rispetto a un asse di simmetria e i parametri dinamici quali sway path e sway area. Alcuni esercizi si sono dimostrati più efficaci nel valutare una diversa strategia di controllo posturale tra gruppo di controllo e pazienti con linfedema: l'appoggio unilaterale, il reaching frontale e il reaching laterale. Inoltre, il parametro sway path si è rivelato il più efficace nel discriminare tra l'esecuzione dell'esercizio con gli occhi aperti e gli occhi chiusi. Per i pazienti con linfedema, il peggioramento della propriocezione può essere una possibile conseguenza del trattamento tumorale, quindi l'analisi proposta può essere utile per valutare gli effetti della terapia. In futuro, per convalidare queste conclusioni sarebbe opportuno utilizzare un campione di dimensioni maggiori.

Per quanto riguarda la struttura di questa tesi, il Capitolo 1 spiega in dettaglio cos'è il linfedema e quali trattamenti sono convenzionalmente eseguiti. Inoltre, vengono presentati i metodi

riportati in letteratura per valutare il controllo posturale a partire dal segnale del CoP. Successivamente, il Capitolo 2 descrive i partecipanti, gli strumenti utilizzati, il protocollo per acquisire i segnali di interesse e l'algoritmo di analisi dei dati. Quest'ultimo è diviso in due parti, analizzando rispettivamente i dati provenienti dal sistema optoelettronico e dalla piattaforma di forza. Il Capitolo 3 riporta i risultati ottenuti, il Capitolo 4 fornisce una discussione e, infine, il Capitolo 5 riassume le conclusioni di questo studio.

CONTENTS

1 INTRODUCTION

1.1 Lymphedema: causes, progression and treatments

Lymphedema is a condition of localized swelling caused by a failure of the lymphatic system. As well as defending the body against infection through lymphocytes, the lymphatic system helps to maintain fluid balance in the body. When blood reaches the capillaries, a portion of plasma escapes and a percentage of it, along with the particulate matter, accumulates in the interstitial space. The lymphatic system removes this excess fluid and these materials from the tissues and returns them to the bloodstream via the lymphatic vessels.

Inadequate lymphatic drainage can have several causes: a congenital dysfunction of the lymphatic system (primary lymphedema) or acquired obliteration such as after radical operative dissection (e.g., extensive axillary or retroperitoneal node removal), radiotherapy, neoplastic disease, or traumatic injury (secondary lymphedema) [1]. In all cases there is a reduction in lymphatic transport and the accumulation of substances in the extracellular space causes swelling. In the specific case of breast cancer, axillary lymphadenectomy is performed to prevent metastasis, but may result in swelling of the upper extremities, trunk, or breasts. The incidence of lymphedema following mastectomy and radiotherapy is ~30% [1].

Lymphedema can be acute, transient, or chronic. Most members of the International Society of Lymphology agree to classify a limb with lymphedema into three stages, recognizing Stage 0, which refers to a condition in which lymphatic transport is impaired, but the swelling is not yet apparent. This latent stage can be transient and can last for months or years. In Stage I, there is an initial accumulation of fluid, but as the limb is elevated, the swelling may decrease. In this first stage, under the pressure from the fingers, a dimple forms in the affected area, which fills as the limb is elevated (pitting). In Stage II there are more changes in the solid structures, the swelling is barely reduced by elevation of the limbs alone, and pitting is present. In Stage III, lymphostatic elephantiasis develops, therefore edema is hard due to tissue fibrosis, pitting may be absent and skin changes may develop [2].

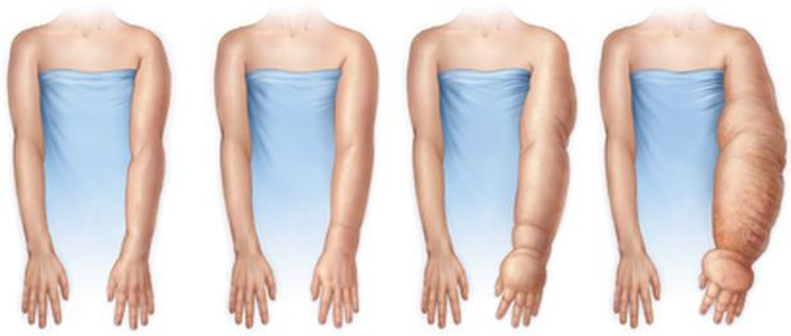

Figure 1.1 Stages 0, I, II, III of upper limb lymphedema [3].

Lymphedema is a debilitating condition that has a slow and progressive course, and if not treated early, can lead to progressive disability: untreated lymphedema may cause chronic inflammation, cellulitis, pain, fatigue, aesthetic deformity, a significant loss of limb mobility and functionality [4]. Peripheral lymphedema can be treated by conservative (non-operative) or operative methods. Basic conservative therapy is used first and then, if this is not sufficient to control the symptoms, surgery should be used. It is important to emphasize that careful hygiene and skin care (cleansing, low pH lotions, emollients) are essential for a successful treatment as well as a good patient education and training. In addition, muscle pumping exercises are very useful, including movements of the limbs performed in everyday activities [2]. The basic conventional therapy recognized as the most effective approach is called Complete Decongestive Therapy (CDT) and consists of two phases: the first one involves attentive skin care, manual lymphatic drainage, multilayer non elastic compression bandaging, exercises and therapeutic education; the second one aims to maintain and optimize the results achieved in the first phase and consists of self-massage and the use of compression garments. To maintain lymphedema reduction after CDT, custom made elastic garments are essential for long-term care. The greatest benefits are achieved with the higher pressure that the patient can tolerate (~20-60 mmHg) [2].

Therapeutic exercises can also be performed in an aquatic environment. To understand the benefits of water for patients with lymphedema, it is advisable to consider its chemical and physical properties. Firstly, the effect of the hydrostatic pressure of the water can help to reduce the limb swelling by stimulating the lymphatic circulation. Secondly, muscular activation and joint mobilization are both improved as part of the gravitational load is eliminated in an aquatic environment. This can help to minimize the effects of prolonged fatigue which characterizes the oncology patient. Finally, water can improve the patient's skin condition. A review conducted by *Maccarone et al.* [1] reports the effects of aquatic exercise on pain, limb motor

function, quality of life (QoL), and limb volume in patients with primary and secondary upper and lower limb lymphedema. The lymphedematous limb strength, the pain perception, the shoulder range of flexion, external rotation, and abduction were shown to improve after performing an aquatic exercise protocol. It also appeared to improve QoL in the study group while, on the contrary, in patients with lymphedema who did not do exercises in water the QoL tended to worsen over time. Regarding the effects on the volume of lymphedematous limb, the majority of studies reviewed showed a reduction, especially in the short term. It should be noted that not all patients (particularly those with wounds or skin disease) are candidates for aquatic therapy.

Another conservative approach to consider is thermal therapy. Studies have shown that the skin temperature rises slowly under bandaging, and it is suggested that this lower-level thermal therapy is helpful. Some centers use far infrared light as an adjunct to bandaging and report improved outcomes [2]. Given the benefits of heat, the exercises performed in thermal water could lead to greater benefits. The positive effects of thermal water therapy on orthopedic patients are already known. However, there is currently little evidence on the outcomes of thermal therapy for lymphedema patients, so the goal is to increase the possibility of this treatment also for cancer patients.

1.2 Center of pressure analysis to quantify postural control

The study of postural control is essential to detect imbalances due to the onset of disease, to identify possible risk factors or to evaluate the effectiveness of a therapy. Postural control is often quantified by recording the trajectory of the Center of Pressure (CoP). In the human body, the CoP refers to the point of application of the ground reaction force vector, which is the force exerted by the ground on a body in contact with it. It is essentially the point at which the total force can be considered to act and it plays a crucial role in maintaining balance and stability during various activities. The CoP trajectory is recorded using force platforms that track the point of application of the ground reaction forces generated under the feet. Typically, the resulting signal is analyzed in terms of either its one-dimensional variations in the medio-lateral (ML) or antero-posterior (AP) directions or its two-dimensional trajectory. There are many areas of application for the CoP study: in sport, especially in disciplines that require a high level of body control and balance, it can provide useful information for optimizing technique and improving athletes' performance; in research into the prevention of falls, especially in the

elderly, it can help identify risk factors and develop prevention strategies; in the field of rehabilitation and physiotherapy, it allows the assessment and improvement of balance and stability in patients with musculoskeletal, neurological or vestibular disorders.. Regarding the topic of our interest, the study by *Hsieh et al.* [5] systematically reviewed and quantitatively synthesized the scientific evidence on gait and balance impairments in breast cancer survivors (BCS) compared to those who never had breast cancer. Research shows that earlier studies focused more on clinical measures, such as the functional reach task or timed up and go (TUG), to assess the quality of life and fatigue [6]. More recent studies have begun to investigate and objectively measure changes in gait and balance as they correlate with impairment, for example measuring CoP speed, CoP displacement, CoP 95% confidence ellipse area and sway area [7] [8] [9]. The results in the group of BCS compared to normative values indicate potential balance and gait impairment in BCS. In addition, BCS demonstrated worse stability in exercises that required greater use of proprioception, i.e., exercises with eyes closed [10] [11]. For instance, some studies have found greater CoP speed in BCS compared to those who have never had breast cancer without visual feedback during a standing balance task. The findings suggest that BCSs rely heavily on visual feedback to maintain upright posture, which may be due to the loss of proprioception often seen after cancer treatment. Proprioception plays a crucial role in postural control by providing information about the position of body parts in space, in order to activate appropriate muscle responses to counteract destabilizing forces and keep the center of mass stable. When the eyes are open, subjects rely more on visual information and less on proprioception. For this reason, it may be useful to assess static balance in the upright position with both eyes open and closed.

Postural control can be quantified using static and/or dynamic posturography tests. Static posturography requires the subject to be in a static position without significant imbalance, while dynamic posturography requires the presence of external or voluntary postural perturbations in order to measure the postural response to these stimuli [12]. Dynamic balance tests are mainly used to assess the risk of falling in the elderly or in people with neurological or musculoskeletal disorders. Studies of postural control in people with lymphedema have mainly used static balance exercises [5]. Only one study [4] used the Limit of Stability Test to assess the ability to shift their center of gravity beyond their basis of support in different directions without losing balance.

A review by *Quijoux et al.* [13] proposed a compendium of definitions of the CoP variables that are the most commonly found in the literature. This study focuses on the comparison between elderly fallers and elderly non-fallers, but among the parameters considered there are also those used to assess postural control in subjects with lymphedema. The calculation of most

of the parameters used in this thesis follows this review. The variables, whose calculation method is described in detail in Paragraph 2.4.2, are mainly of two types:

- Positional variables, which describe the dispersion characteristics of the trajectory and do not require knowledge of the signal dynamics; they are for example the average and maximum distance, the oscillation range and the confidence ellipse at 95%.
- Dynamic parameters, which are based on the dynamics of the CoP and require knowledge of local displacements, such as sway path and sway area.

1.3 Aim of the thesis

The aim of this thesis is to study postural control during functional tasks of the upper limb by analyzing the CoP signal. In particular, based on the parameters of the CoP proposed in the state-of-art literature, we want to analyze the performance of a control group compared with that of patients with lymphedema. After evaluating whether the results are consistent with the literature, we want to identify if some parameters differ between patients and controls, or if some tasks are more effective in evaluating a different postural control strategy between the control group and patients with lymphedema, to propose an acquisition and processing protocol that can be used in a clinical setting.

2 MATERIALS AND METHODS

2.1 Participants

Eleven healthy women aged 21-51 were included as a control group. In addition, two women, aged 53 and 55, who were diagnosed with lymphedema in the arm following breast cancer removal took part in the study. All participants gave written informed consent to the study. Information such as age, weight, height, dominant limb and, in the case of patients, which limb was affected by lymphedema was collected from each participant. Table 2.1 summarizes all this information as *median [minimum value - maximum value]* for the control group and individually for the two participants with lymphedema.

	CONTROL GROUP (11 participants)	**LYMPHEDEMA GROUP (2 participants)**	
		Lymp001	**Lymp002**
Age [years]	27 [21-51]	55	53
Height [cm]	169 [160-180]	160	164
Weight [kg]	60 [50-85]	115	62
Dominant limb	9 right - 2 left	right	right
Limb with lymphedema	/	right	right

Table 2.1 Characteristics of study participants.

2.2 Acquisition system

In this study, an optoelectronic system (Vicon Vero, sampling frequency of 100 Hz) integrated with a force platform (Bertec Model 4060-10, sampling frequency of 2000 Hz) was used to obtain information on the kinematics and dynamics of the human body. Data were collected using Vicon Nexus software for offline processing.

Markers (see Figure 2.3b) placed on the participant's body surface are made of reflective material capable of reflecting the light generated near the cameras. The cameras (see Figure 2.3a) detect the reflected light and the acquired data is processed by software capable of calculating the three-dimensional position of the markers over time. The spherical retro-reflective markers were placed over prominent bony landmarks [14]. Table 2.2 describes the markers used in this study and Figure 2.1 shows their placement on the participant's body.

Marker Label	Definition	Position on the participant
RELB	Right elbow	On the lateral epicondyle
LELB	Left elbow	On the lateral epicondyle
RHEE	Right heel	On the calcaneus at the same height above the plantar surface of the foot as the toe marker
LHEE	Left heel	On the calcaneus at the same height above the plantar surface of the foot as the toe marker
RTOE	Right toe	Over the second metatarsal head, on the midfoot side of the equinus break between forefoot and midfoot
LTOE	Left toe	Over the second metatarsal head, on the midfoot side of the equinus break between forefoot and midfoot

Table 2.2 Definition and description of the positioning of the markers used.

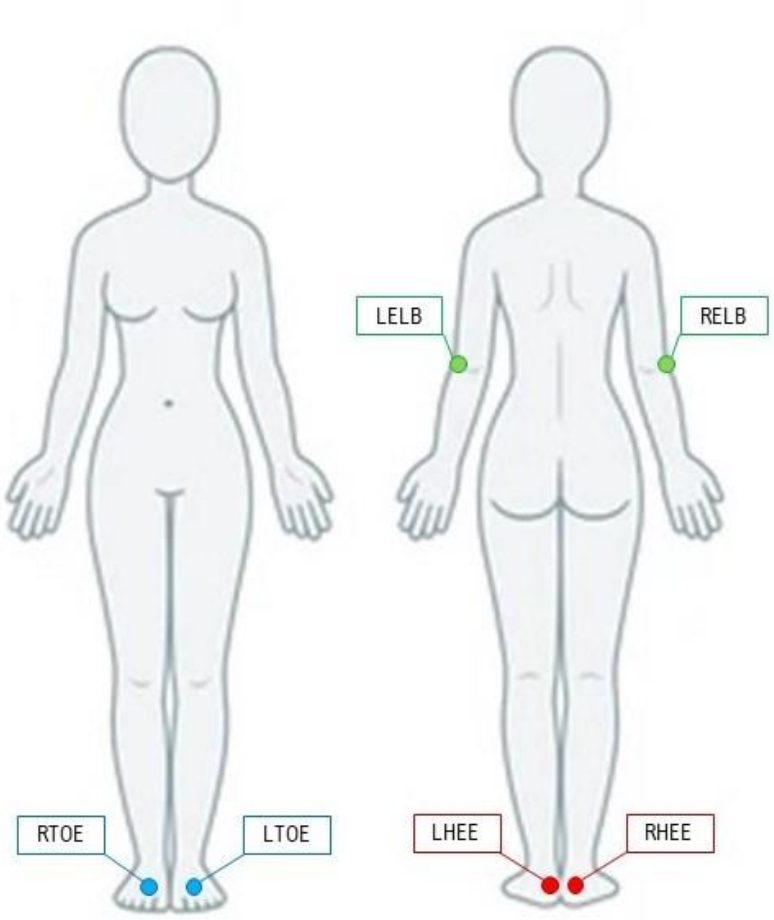

Figure 2.1 Visualisation of marker placement in the human body.

In particular, RELB/LELB markers were used to detect the start and end times of repetitions in upper limb functional tasks. The markers on the feet were used to calculate position parameters during bilateral stance and, in addition, RHEE/LHEE were used to identify the beginning and end of each repetition during unilateral stance.

A calibration procedure was executed before the first data acquisition. To calibrate the cameras, a calibration wand (see Figure 2.3c) was waved over the area where 3D data will be acquired. To set the volume origin, the calibration object was placed flat on the ground in the position and orientation of the origin of the global coordinate system.

In this thesis, the origin of the global reference system, for both the optoelectronic system and the force platform, was located on the corner of the force platform. The orientation of the reference system is shown in Figure 2.2: the x, y and z axes represent the medio-lateral, antero-posterior and vertical directions respectively.

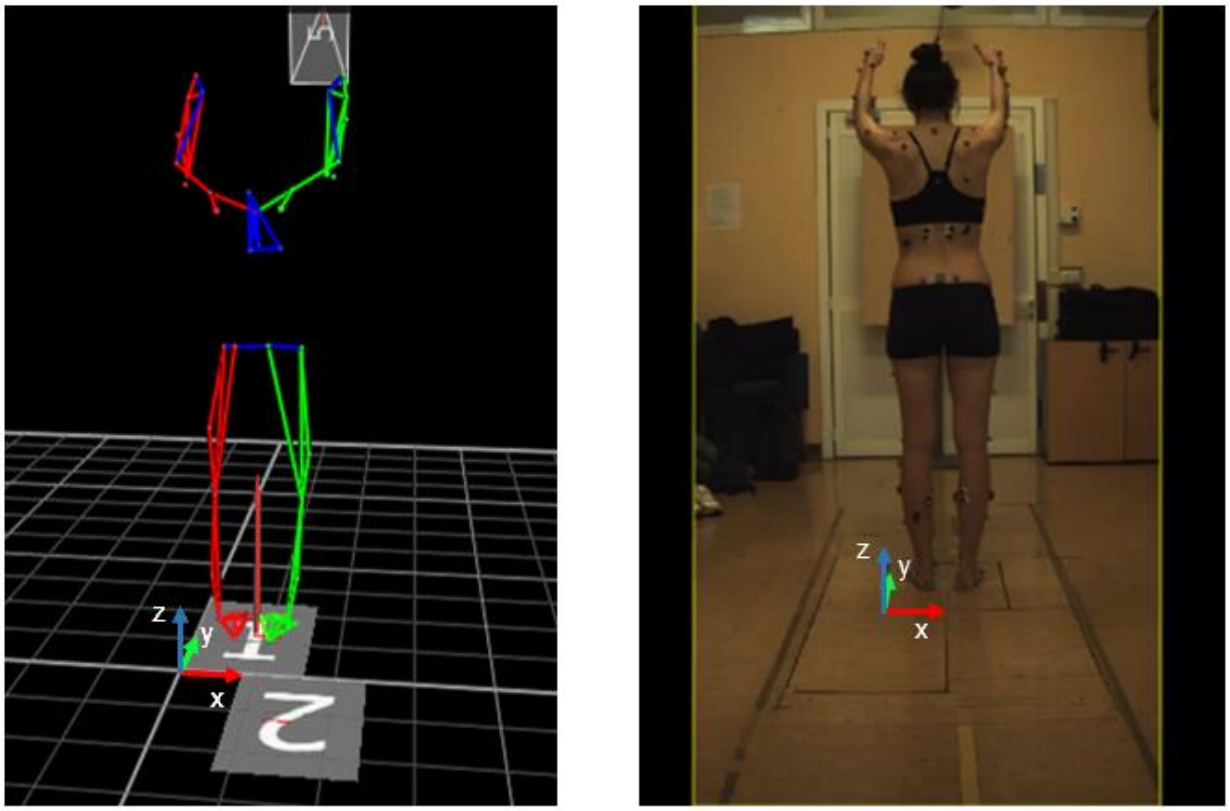

Figure 2.2 Orientation of the global reference system for both the optoelectronic system and the force platform: the origin is located on the corner of the force platform and the x, y and z axes represent the medio-lateral, antero-posterior and vertical directions respectively.

Force platforms (see Figure 2.3d) are devices consisting of a rectangular instrumented plate capable of measuring the three components of the resultant forces and torques applied with respect to a local reference system defined on the platform. They have built-in force sensors that are sensitive to changes in pressure or compression. These sensors can be based on different technologies, such as piezoelectric load cells or strain gauges, which produce electrical signals proportional to the force applied: the strain gauges are bonded to an elastic element that deforms following a load and this change in length affects the electrical resistance which is measured through an electrical circuit. In the case of piezoelectric sensors, they produce a proportional electric charge as a result of load, which can be converted by an amplifier into an easily measurable output voltage.

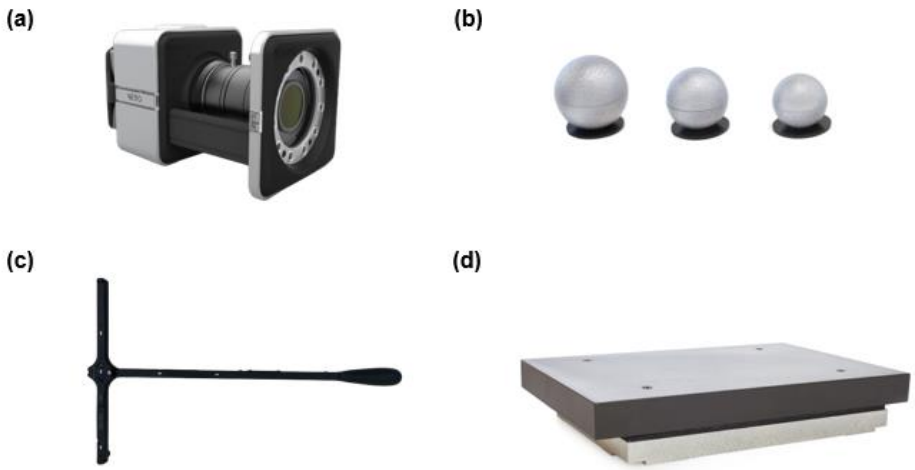

Figure 2.3 Equipment used for data acquisition: (a) camera of the optoelectronic system [15]; (b) reflective markers [16]; (c) calibration wand [17]; (d) force platform [18].

The force platform is connected to a computer which records the displacement of the CoP, forming the CoP signal. It is generally represented in two ways: a *stabilogram*, a plot of the CoP time series in one direction, either medio–lateral (Figure 2.4a) or antero–posterior (Figure 2.4b); a *statokinesigram*, a plot of the CoP displacement in the horizontal plane, obtained by plotting the antero-posterior displacement as a function of the medio-lateral displacement (Figure 2.4c).

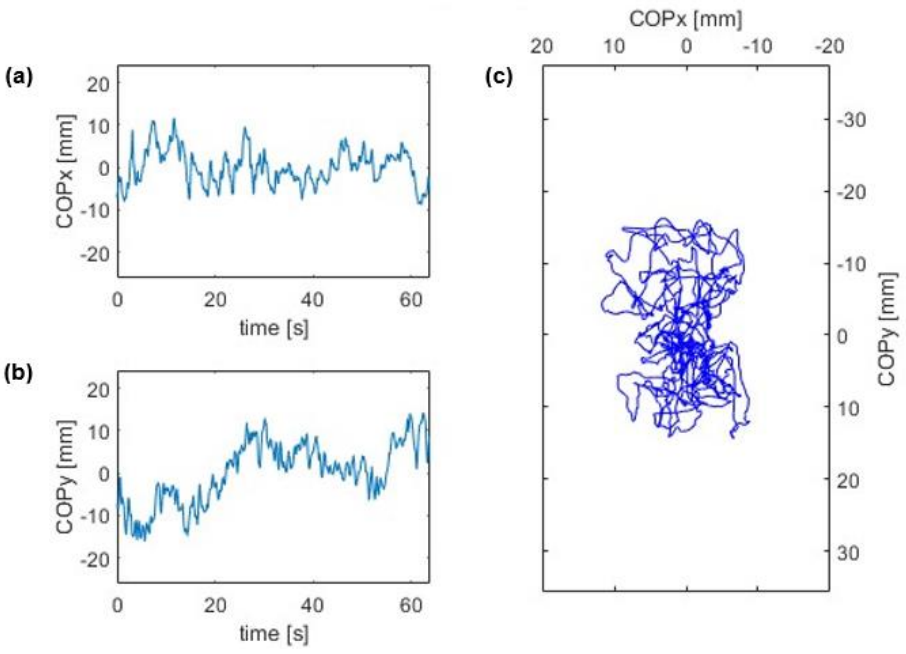

Figure 2.4 CoP displacement of a representative participant (Contr008) during bilateral stance with eyes open: mono-dimensional time series in ML direction (a) and AP direction (b); two-dimensional CoP trajectory in the horizontal plane (c).

2.3 Tasks

The participants were instructed to complete the following series of tasks. The starting position for each task was to stand barefoot with both feet on the force platform (at a self-selected distance between the feet) and with arms outstretched at the sides. For all of the exercises described below, except the bilateral stance, the participant performed three repetitions of each task with a few seconds of rest in between.

- **Bilateral Stance 60 s**: The participant was instructed to remain still for 60 s. This task is performed first with eyes open (**EO**), looking straight ahead at a visual target, and then with eyes closed (**EC**).
- **Unilateral Stance x3 10 s**: The participant was instructed to lift one foot to balance on the opposite leg for 10 s; between each repetition the participant places both feet back on the platform for a few seconds; it is performed first with the right leg (**dx leg**) and then with the left leg (**sn leg**).
- **Frontal Elevation x3**: The participant was instructed to raise the arms in the sagittal plane, bringing them up to 180° before lowering them back to the resting position. The task was performed by raising both arms simultaneously (**both arms**).
- **Scapular Elevation x3**: The participant was instructed to raise the arms in the scapular plane (i.e., approximately 45° plane from the sagittal plane), raise them 180° and lower them back to the resting position. The task was performed by raising both arms simultaneously (**both arms**).
- **Frontal Reaching x3**: The participant was instructed to move the arms in front of her/him as to reach an object at shoulder height and to lower them back to the resting position. The task was performed with each arm separately (**dx/sn arm**) as well as with both arms together (**both arms**).
- **Lateral Reaching x3**: The participant was instructed to move the arms laterally as to reach an object placed laterally at shoulder height and to lower them back to the resting position. The task was performed with each arm separately (**dx/sn arm**) as well as with both arms together (**both arms**).
- **Upward Reaching x3**: The participant was instructed to move the arms above the head as to reach an object placed above them and to lower them back to the resting position. The task was performed with each arm separately (**dx/sn arm**) as well as with both arms together (**both arms**).

- **Circumduction x3**: The participant was instructed to perform a complete circumduction with the arms by carrying them forward and then backward. The task was performed with each arm separately (**dx/sn arm**) as well as with both arms together (**both arms**).

2.4 Data analysis

Data analysis was performed in a MatLab environment (MATLAB R2023a). The first part consists of the analysis of the data from the optoelectronic system for the segmentation of the movement: the purpose is to identify the temporal moments in which the arm movement begins and ends, in order to identify the periods of interest for the analysis of the Center of Pressure (CoP) signal. Consequently, the second part involves processing the CoP data from the force platform in order to obtain useful posturographic parameters.

2.4.1 Movement segmentation algorithm

We first describe the movement segmentation procedure in the upper limb functional tasks and then move on to unilateral stance.

To characterize postural control during the upper limb functional tasks, data from the optoelectronic system were used to identify the time intervals during which the participant performed the task. Therefore, the first step was to create an algorithm that identifies the moments of start and end of each repetition of the task.

The most suitable markers for this purpose are those placed on the elbows at the lateral epicondyle (LELB/RELB), as they best indicate the movement of the upper arm. Those placed laterally rather than medially were chosen because they are often occluded in the latter case. Figure 2.5 shows an example of the RELB marker during a frontal reaching task with the right arm.

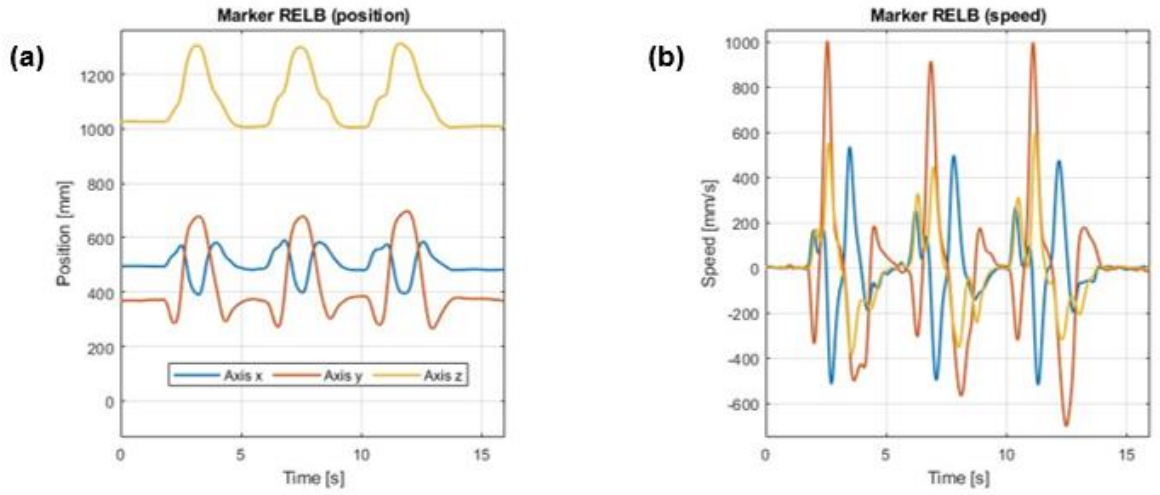

Figure 2.5 Plot of position (a) and speed (b) as function of time in the three directions of the RELB marker in a representative participant (Contr003) during Frontal Reaching (dx arm). The blue, red and yellow curves refer respectively to the x, y, z axes that conventionally represent the transverse, sagittal and longitudinal axes of the human body.

The time intervals in which the participant does not move are characterized by values of speed and displacement with respect to the initial position close to zero, so the goal was to look for a threshold value below which these conditions would occur. First, the instantaneous speed (s) was calculated as the derivative ($\delta \cdot$) of position (p) with respect to time (t):

$$s = \frac{\delta p}{\delta t} \tag{1}$$

The calculation was performed for the three position components p_x, p_y, p_z, therefore the speed was obtained in the three directions: s_x, s_y, s_z. Then, to obtain the resultant of the three directions of both position and speed, the Pythagorean Theorem was applied in the three directions:

$$p = \sqrt{{p_x}^2 + {p_y}^2 + {p_z}^2} \tag{2}$$

$$s = \sqrt{{s_x}^2 + {s_y}^2 + {s_z}^2} \tag{3}$$

Figure 2.6 shows the resulting position and instantaneous speed of the RELB marker in the case of frontal reaching task with the right arm.

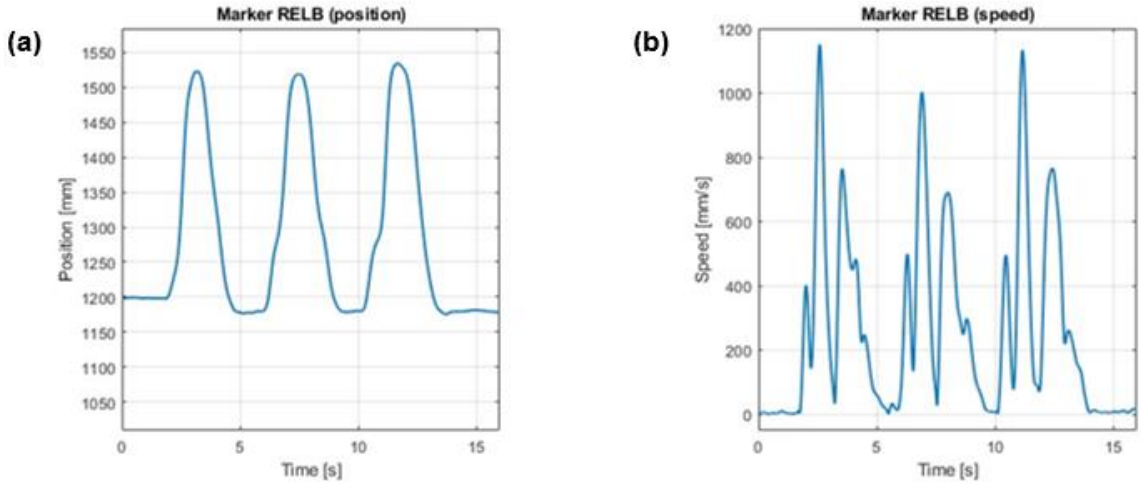

Figure 2.6 Plot of position (a) and speed (b) result as function of time of the RELB marker in a representative participant (Contr003) during Frontal Reaching (dx arm).

By sliding a time window of 50 ms along the entire signal without overlapping, the root mean square (RMS) was calculated for each window as follows:

$$RMSp = \sqrt{\frac{1}{N}\sum_{i=1}^{N} p_i^2} \quad (4)$$

$$RMSs = \sqrt{\frac{1}{N}\sum_{i=1}^{N} s_i^2} \quad (5)$$

where N is the total number of samples in a window. At this point, we calculated the logarithm of the RMS for both position and speed and with the resulting data vectors we obtained two histograms (see Figure 2.7). By applying a Gaussian smoothing to the histogram, we obtained a curve f which showed a recurring trend between the different participants and tasks: we can see two bell-shaped peaks, the first at generally low values (see the area highlighted in red in the graphs in Figure 2.7) and the second at higher values (see the area highlighted in blue in the graphs in Figure 2.7). In the histogram relating to the speed (Figure 2.7b) this trend is much clearer. It can be seen that in both graphs the first bell contains the values relating to the rest

intervals, so by identifying the last point of it we can obtain the threshold below which the position and speed are low. To do this, we first found the maximum point of the first bell of f. At this point, to determine the end of the bell, we wanted to find the point at which f has a local minimum, i.e., the point where the first derivative is zero and the second derivative is positive. We obtained the curves f' and f'' calculating its first and second derivative. Starting from the corresponding point of the local maximum just identified, we looked for the first zero crossing of f' and we verified that at this point f'' was positive. By calculating the exponential of the value just found (for the example in Figure 2.7 it is $10^{3.0932}$ for the position and $10^{1.448}$ for the speed) we obtained the threshold we were looking for.

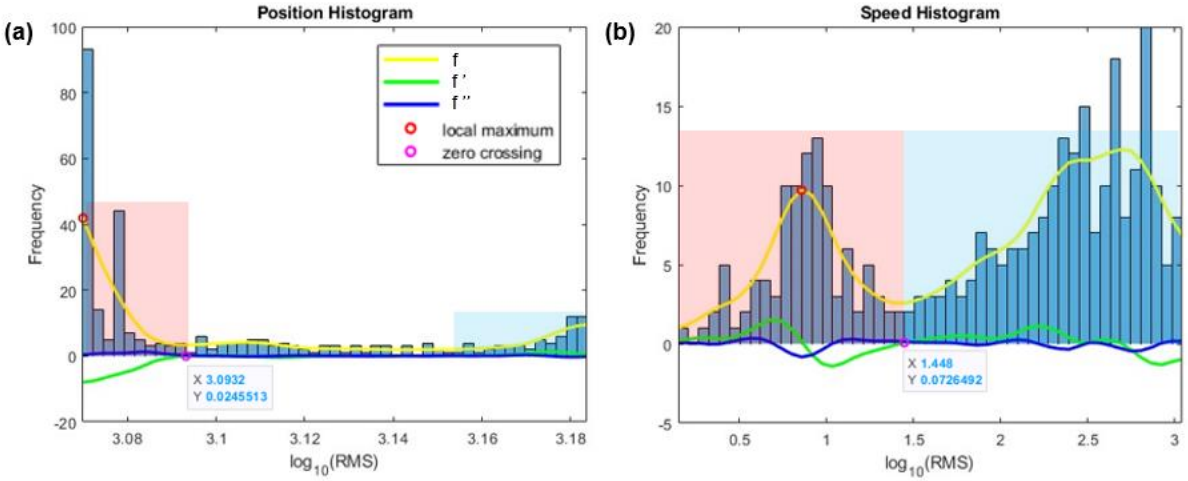

Figure 2.7 Histogram of the RMS logarithm of position (a) and speed (b) of the RELB marker in a representative participant (Contr003) during Frontal Reaching (dx arm). The yellow curve (f) represents the result of a gaussian smoothing. The green curve (f') is the first derivative of f and the blue curve (f'') is the second derivative of f. The red rectangles identify the first bell-shaped curve at low values, while the blue ones identify the second bell-shaped curve at higher values. The red circle is the local maximum of f in the first bell. The pink circle is the first zero crossing of f after the local maximum. In this case the values obtained from the graph are 3.0932 for the position and 1.448 for the speed. By applying the logarithm to these values, the thresholds of interest are obtained.

At this point, the time when the position and speed values were simultaneously below the respective thresholds were considered to determine the rest intervals. Inevitably, the participant was not perfectly stationary between repetitions, so there may be short time intervals that are identified as movement when in fact they refer to small movements that are not of interest to us. In order to eliminate them, the length of these intervals is calculated and only the longest ones are kept, in particular in number corresponding to the number of movement repetitions.

The temporal instants of start and end of each repetition were obtained as described above. When the movement was performed with a single arm, the analysis was carried out on the single corresponding marker. When the movement was performed with both arms, the analysis was performed separately on the markers of the two arms and then, in order to determine the movement intervals, the smallest between the start times and the largest between the end times were considered. Figure 2.8 shows an example of movement segmentation in a frontal reaching task with the right arm.

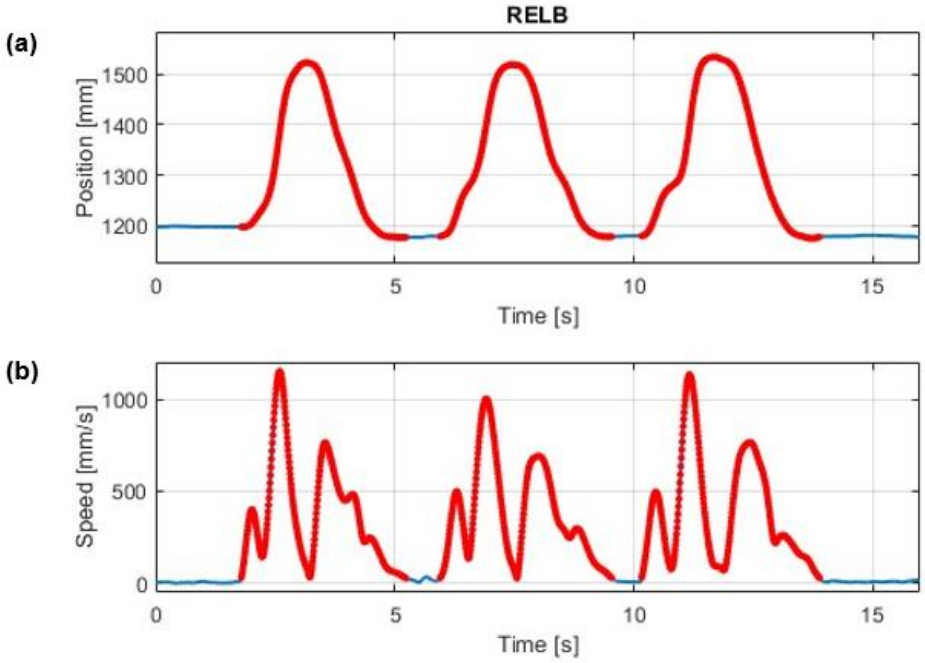

Figure 2.8 Movement segmentation on position (a) and speed (b) of the RELB marker in a representative participant (Contr003) during Frontal Reaching (dx arm). In red the movement intervals are represented.

For a unilateral stance, it is important to extract the time intervals in which the participant is in monopodal balance. The segmentation algorithm is the same as for the upper limb functional tasks, but it is useful to make some observations.

The most appropriate marker for this purpose was the one placed on the heel of the foot that was lifted during the task: LHEE if the unilateral stance was performed on the right side or RHEE if it was performed on the left side. Observing the trend of position and speed both in the three components (Figure 2.9) and in the resulting one (Figure 2.10), it seems easier to look for the start and end moments of the movement in the z-component of position and speed.

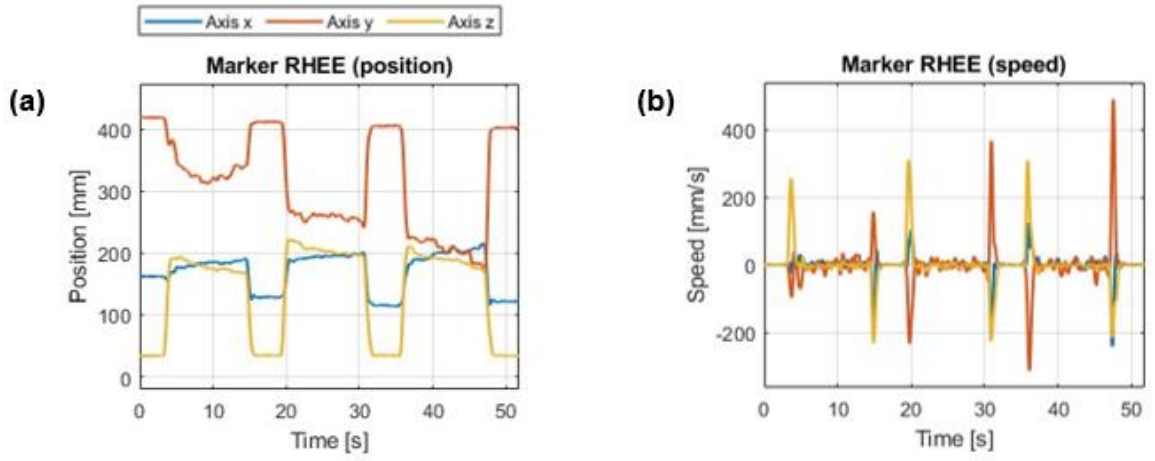

Figure 2.9 Plot of position (a) and speed (b) as function of time in the three directions of the RHEE marker in a representative participant (Contr007) during Unilateral Stance (sn leg). The blue, red and yellow curves refer respectively to the x, y, z axes that conventionally represent the transverse, sagittal and longitudinal axes of the human body.

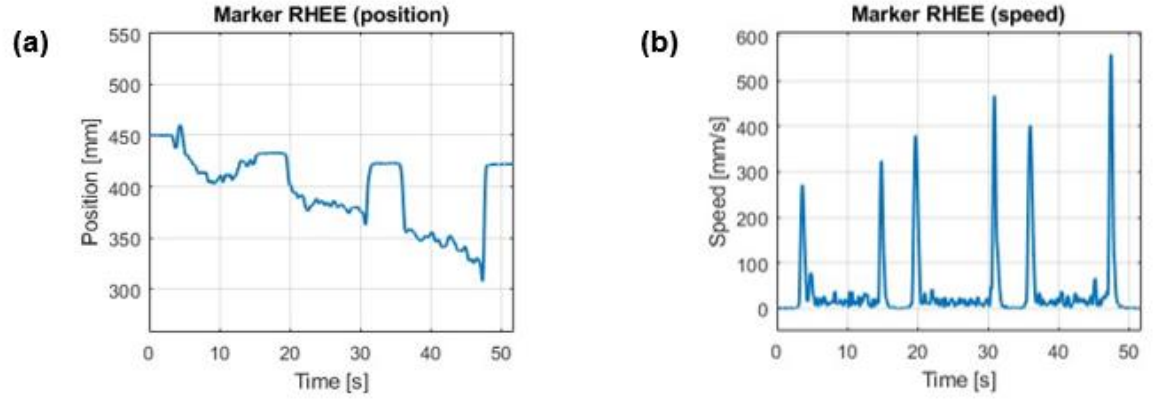

Figure 2.10 Plot of position (a) and speed (b) result as function of time of the RHEE marker in a representative participant (Contr007) during Unilateral Stance (sn leg).

As before, we calculated the RMS, took the logarithm and calculated the histogram (see Figure 2.11). In this case we can see that in terms of position (see Figure 2.11a) the trend is similar to what we saw before, while in the f curve of the speed graph (see Figure 2.11b) there is a single large bell-shaped curve. This is due to the fact that the temporal moments when the speed is almost zero are, in addition to those of the rest zones, also those of the monopodal balance. We therefore identified the position and speed thresholds by taking the values corresponding respectively to the end of the first bell in the position curve, using the procedure seen previously, and to the only bell in the speed curve. In this way, the values below the speed threshold corresponded to the intervals of our interest, but also to the rest zones. The latter occur at values below the position threshold therefore it was sufficient to exclude these instants from those identified with the speed and thus we obtained the intervals of our interest.

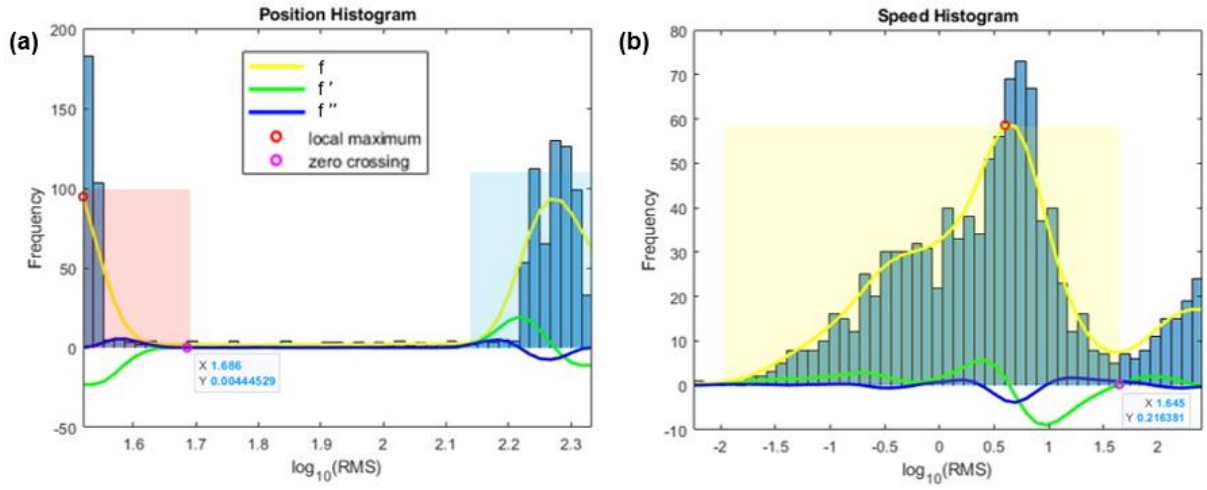

Figure 2.11 Histogram of the RMS logarithm of position (a) and speed (b) of the RHEE marker in a representative participant (Contr007) during Unilateral Stance (sn leg). The yellow curve (f) represents the result of a gaussian smoothing. The green curve (f') is the first derivative of f and the blue curve (f'') is the second derivative of f. In the position graph the red rectangle identifies the first bell-shaped curve at low values, while the blue curve identifies the second one at higher values. In the speed graph the orange rectangle identifies the only bell-shaped curve. The red circle is the local maximum of f in the first bell. The pink circle is the first zero crossing of f after the local maximum. In this case the values obtained from the graph are 1.686 for the position and 1.645 for the speed. By applying the logarithm to these values, the thresholds of interest are obtained.

Figure 2.12 shows an example of segmentation where monopodal stance intervals are highlighted.

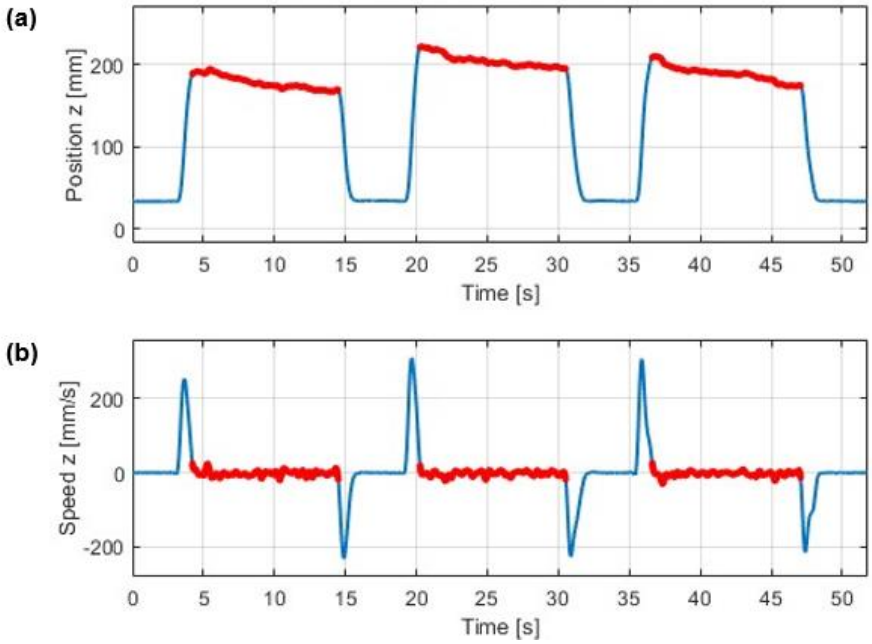

Figure 2.12 Movement segmentation on position (a) and speed (b) along the z axis of the RHEE marker in a representative participant (Contr007) during Unilateral Stance (sn leg). In red the intervals of monopodal stance are represented.

2.4.2 CoP data processing

We start by describing the parameters calculated to assess the postural control strategy in a bilateral stance, and then move on to unilateral stance and upper limb functional tasks (most of the indices/parameters described below are taken from the review of *Quijoux et al.* [13]).
The CoP time series were passed through a fourth-order zero phase Butterworth low-pass filter with a 12,5 Hz cut-off frequency. We indicated the two CoP time series along the medio-lateral and antero-posterior directions respectively as CoP_{ML} and CoP_{AP}. It was assumed that the CoP trajectory contained N data points, sampled at the frequency Fs. The average position in the two directions was calculated as the arithmetic mean of the trajectory of CoP_{ML} and CoP_{AP}:

$$Mean_{ML} = \frac{1}{N}\sum_{n=1}^{N} CoP_{ML} \quad (6)$$

$$Mean_{AP} = \frac{1}{N}\sum_{n=1}^{N} CoP_{AP} \quad (7)$$

First of all, we calculated the positional parameters, which do not depend on the dynamics of the CoP and which express the dispersion of the trajectory.
The first parameter is the distance of the mean CoP with respect to the straight line passing through the midpoint of the markers on the heels (RHEE/LHEE) and the midpoint of the markers on the second metatarsals (RTOE/LTOE). We can see a representation in Figure 2.13. Assuming that M was the number of marker data points, we calculated the coordinates of these two central points, named as HEE and TOE, as the mean of the left and right marker coordinates. The subscripts x and y refer to the components of the markers along the medio-lateral and antero-posterior directions, respectively.

$$HEEx = \frac{1}{M}\sum_{m=1}^{M} \frac{RHEEx_m + LHEEx_m}{2} \quad (8)$$

$$HEEy = \frac{1}{M}\sum_{m=1}^{M} \frac{RHEEy_m + LHEEy_m}{2} \quad (9)$$

$$TOEx = \frac{1}{M}\sum_{m=1}^{M} \frac{RTOEx_m + LTOEx_m}{2}$$

(10)

$$TOEy = \frac{1}{M}\sum_{m=1}^{M} \frac{RTOEy_m + LTOEy_m}{2}$$

(11)

To calculate the equation of the line that passes through HEE and TOE we considered the equation of a line in implicit form as

$$ax + by + c = 0$$

(12)

then we calculated the coefficients as follows:

$$a = TOEy - HEEy$$

(13)

$$b = HEEx - TOEx$$

(14)

$$c = TOEx * HEEy - HEEx * TOEy$$

(15)

At this point the distance between the mean CoP, whose coordinates are $(Mean_{ML}, Mean_{AP})$, and the straight line is given by the following formula.

$$MeanCoPDisplacement = \frac{|a * Mean_{ML} + b * Mean_{AP} + c|}{\sqrt{a^2 + b^2}}$$

(16)

To distinguish which side the average CoP was on with respect to the line we assigned to this parameter the negative sign when it tended towards the non-dominant side.

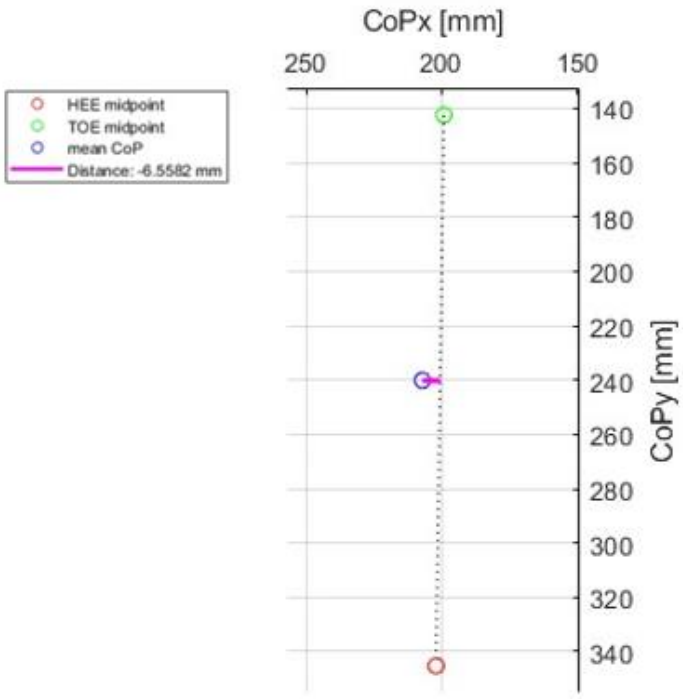

Figure 2.13 MeanCoPDisplacement: distance between the CoP mean point (blue circle) and the line passing through the midpoint of heels markers (red circle) and the midpoint of second metatarsals markers (green circle) in a representative participant (Contr010) during Bilateral Stance with eyes open.

Subsequently, for each $1 \leq n \leq N$, the coordinates of the centered trajectories on the ML axis and AP axis were obtained subtracting respectively $Mean_{ML}$ and $Mean_{AP}$:

$$CoPx_n = CoP_{MLn} - Mean_{ML} \quad (16)$$

$$CoPy_n = CoP_{APn} - Mean_{AP} \quad (17)$$

We also introduced the *Radius signal* (R) computed as the Euclidean distance of the centered CoP to the origin so, for each $1 \leq n \leq N$,

$$R_n = \sqrt{CoPx_n^2 + CoPy_n^2} \quad (18)$$

Using the centered signals, we defined the following parameters:

- *Mean Distance* [mm]: it represents the mean distance of the CoP from the center of the trajectory and it is computed as the average of the absolute value of the signal.

$$MeanDistance_{ML} = \frac{1}{N}\sum_{n=1}^{N}|CoPx_n| \quad (19)$$

$$MeanDistance_{AP} = \frac{1}{N}\sum_{n=1}^{N}|CoPy_n| \quad (20)$$

$$MeanDistance = \frac{1}{N}\sum_{n=1}^{N}|R_n| \quad (21)$$

- *Maximal Distance* [mm]: it represents the maximal distance of the CoP from the center of the trajectory and it is computed as the maximum of the signal.

$$MaximalDistance_{ML} = \max_{1\le n\le N}|CoPx_n| \quad (22)$$

$$MaximalDistance_{AP} = \max_{1\le n\le N}|CoPy_n| \quad (23)$$

$$MaximalDistance = \max_{1\le n\le N}|R_n| \quad (24)$$

- *Range* [mm]: it represents the maximal distance between any two points of the stabilogram. Along one particular axis, it is mathematically equivalent to the distance between the maximum and the minimum positions of the signal.

$$Range_{ML} = \max_{1\le n\le N} CoPx_n - \min_{1\le n\le N} CoPx_n \quad (25)$$

$$Range_{AP} = \max_{1\le n\le N} C0Py_n - \min_{1\le n\le N} CoPy_n \quad (26)$$

- *Range Ratio*: it represents a directional index and it is computed as the ratio of medio-lateral amplitude over the antero-posterior amplitude.

$$RangeRatio = \frac{Range_{ML}}{Range_{AP}}$$

(27)

Subsequently we examined the Confidence Ellipse, that is the smallest ellipse that contains 95% of the points of the CoP trajectory (Figure 2.14). To determine the length and orientation of the main axes of the ellipse we calculated eigenvalues and eigenvectors of the covariance matrix between $CoPx$ and $CoPy$: in fact, the eigenvectors provide information on the directions of the axes while the eigenvalues provide information on the length. The eigenvector corresponding to the largest eigenvalue allows us to calculate the direction in which the greatest data variance is present, therefore the direction of the major axis. The eigenvector corresponding to the minor eigenvalue gives the direction perpendicular to the major axis. Therefore, if we denote the eigenvalues as λ_1 and λ_2, where $\lambda_1 \geq \lambda_2$, and the corresponding eigenvectors as $\begin{bmatrix} v1 \\ v2 \end{bmatrix}$ and $\begin{bmatrix} u1 \\ u2 \end{bmatrix}$, the following parameter was calculated as follows:

- *Major Axis Inclination* [°]: it represents the angle of inclination of the major axis with respect to the ML direction and it is computed as the arctangent of the ratio between the second component of the eigenvector associated with the largest eigenvalue and the first component of that eigenvector.

$$InclinationAngle = \arctan\left(\frac{v2}{v1}\right)$$

(28)

The length of the axis is obtained from the double product of the confidence interval C and the standard deviation σ along the direction of the axis. C is calculated using the Fisher distribution with 2 degrees of freedom for the numerator and (N - 2) degrees of freedom for the denominator, considering a 95% confidence level. σ is equal to the square root of the eigenvalue corresponding to the eigenvector expressing that direction so the parameters were calculated as described below:

- *Major Axis Length* [mm]: it represents the length of the major axis and it is proportional to the square root of the largest eigenvalue.

$$MajorAxisLength = 2 * C * \sqrt{\lambda_1}$$

(29)

- *Minor Axis Length* [mm]: it represents the length of the minor axis and it is proportional to the square root of the smallest eigenvalue.

$$MinorAxisLength = 2 * C * \sqrt{\lambda_2}$$

(30)

- *Axes Lengths Ratio*: it represents a directional index and it is computed as the ratio of the length of the major axes to the minor axes.

$$AxesLengthsRatio = \frac{MajorAxisLength}{MinorAxisLength}$$

(31)

- *Area of the Ellipse* [mm^2]: it represents the area of the confidence ellipse and it is computed as

$$EllipseArea = \pi * \frac{MajorAxisLength}{2} * \frac{MinorAxisLength}{2}$$

(32)

A larger area indicates greater dispersion of the CoP and a less tightly controlled CoP position.

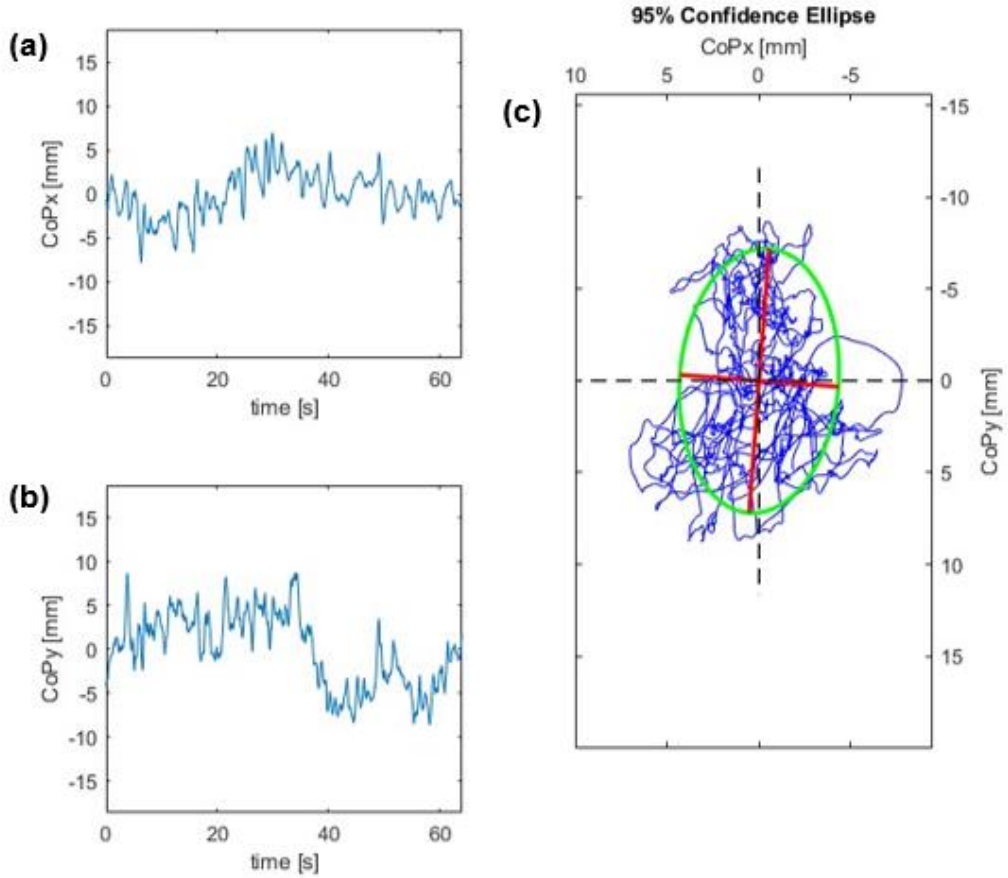

Figure 2.14 CoP displacement of a representative participant (Contr004) during bilateral stance with eyes open: mono-dimensional time series in ML direction (a) and AP direction (b); two-dimensional CoP trajectory in the horizontal plane and representation of the 95% Confidence Ellipse (green curve) with the principal axes (red lines) (c).

Then we calculated the dynamic parameters, therefore based on the local displacements of the trajectory of the CoP.

- *Sway Path* [mm/s]: it is the length of the CoP trajectory normalized to the acquisition duration and it provides insight into the extent of corrective CoP actions taken during a balance task; it corresponds to the average speed of the CoP and it is calculated as

$$SwayPath = \frac{Path}{Acquisition\ Duration} \quad (33)$$

where $Path$ is the sum of the Euclidean distances between consecutive points.

$$Path = \sum_{i=2}^{N} \sqrt{(CoPx_i - CoPx_{i-1})^2 + (CoPy_i - CoPy_{i-1})^2} \quad (34)$$

- *Sway Area* [mm^2/s]: it is the measurement of the surface swept by the ray that connects the midpoint of the trajectory with all the subsequent points of the trajectory itself, normalized to the acquisition duration; it is calculated as

$$SwayArea = \frac{Area}{Acquisition\ Duration}$$

(35)

where $Area$ is calculated by adding the area of the triangles whose vertices are two consecutive points of the CoP trajectory and the mean position of the CoP. The area of a triangle can be expressed as half the absolute value of the determinant of a 3x3 matrix in whose rows the coordinates of the three vertices are indicated:

$$Area = \sum_{i=2}^{N} \frac{1}{2} \left| det \begin{bmatrix} CoPx_i & CoPy_i & 1 \\ CoPx_{i-1} & CoPy_{i-1} & 1 \\ Mean_x & Mean_y & 1 \end{bmatrix} \right|$$

(36)

where

$$Mean_x = \frac{1}{N} \sum_{n=1}^{N} CoPx$$

(37)

and

$$Mean_y = \frac{1}{N} \sum_{n=1}^{N} CoPy$$

(38)

are the mean coordinates of the signal.

- *Sway Area over Sway Path Ratio* [mm]: it is computed as the ratio of the sway area to the sway path.

$$SwayArea/SwayPath = \frac{SwayArea}{SwayPath}$$

(39)

Regarding data processing in unilateral stance and in upper limb functional tasks, after filtering the signals, we extracted the portions of the signal relating to the intervals of interest based on the time instants identified by the segmentation algorithm. For the unilateral stance the intervals in which the participant was in monopodal balance were extracted (see Figure 2.15), while in upper limb functional tasks the ranges of interest extracted were those in which there was movement (see Figure 2.16).

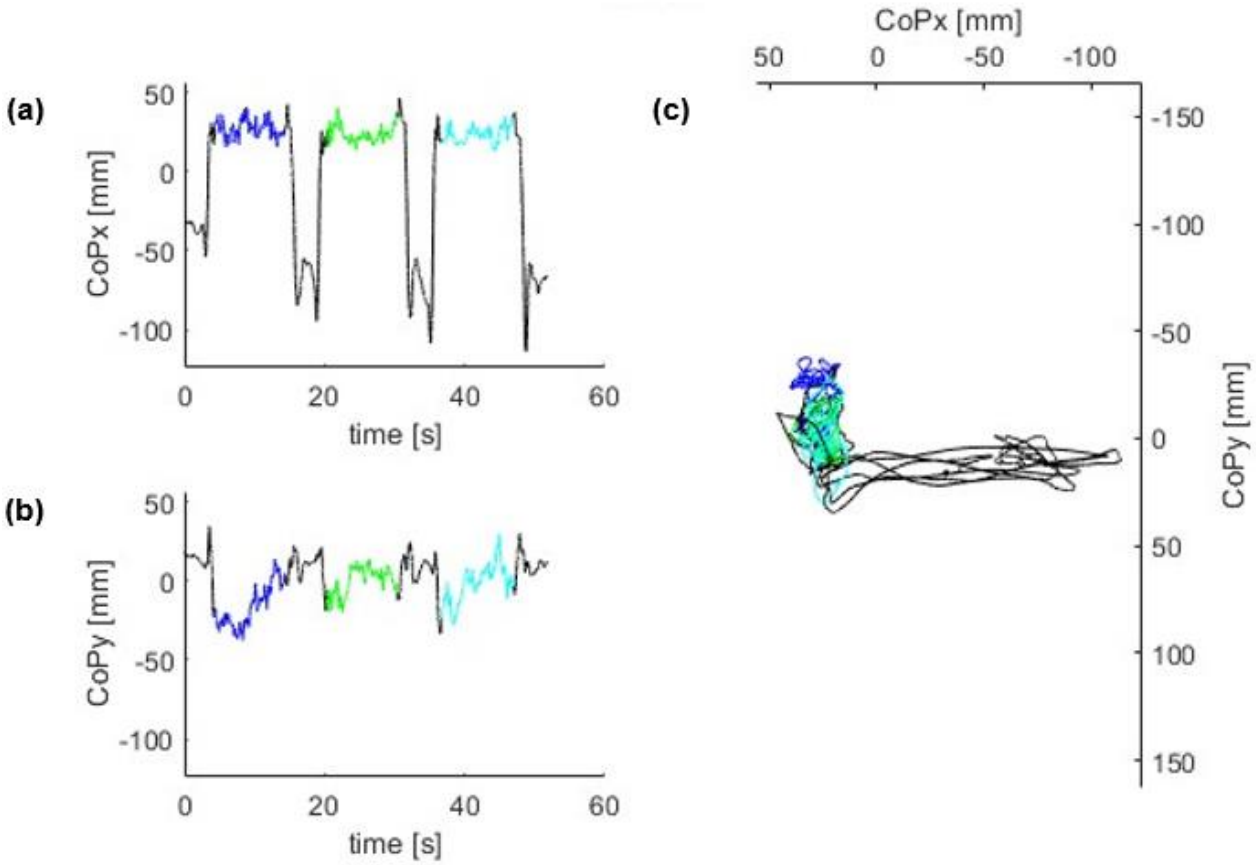

Figure 2.15 CoP displacement of a representative participant (Contr007) during unilateral stance (sn leg): mono-dimensional time series in ML direction (a) and AP direction (b); two-dimensional CoP trajectory in the horizontal plane (c). In different colors the ranges of interest in each repetition are represented.

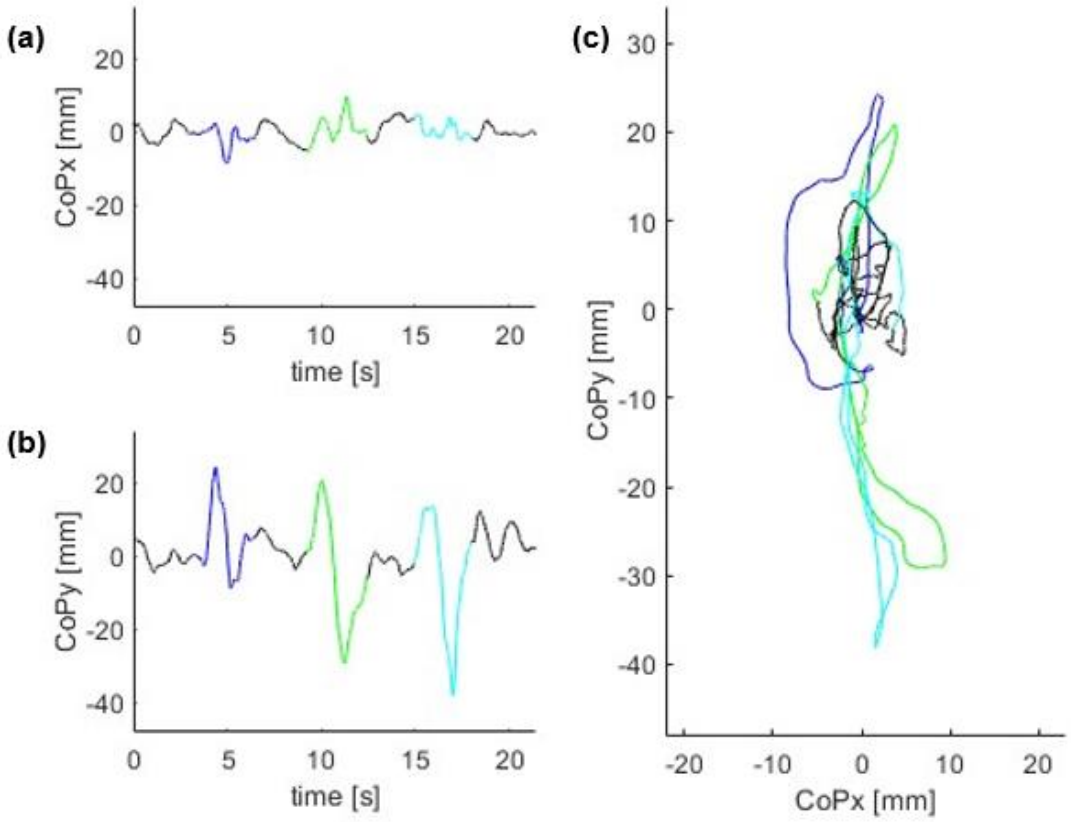

Figure 2.16 CoP displacement of a representative participant (Contr004) during circumduction (both arms): mono-dimensional time series in ML direction (a) and AP direction (b); two-dimensional CoP trajectory in the horizontal plane (c). In different colors the ranges of interest in each repetition are represented.

The parameters calculated to evaluate the postural control in unilateral stance and in upper limb functional tasks were:

- $Range_{ML}$ [mm]
- $Range_{AP}$ [mm]
- $RangeRatio$
- $SwayPath$ [mm/t]
- $SwayArea$ [mm^2/t]
- $SwayArea/SwayPath$ [mm]

The calculation method was the same as described before on the parameters used in bilateral stance. The calculation was performed separately for each segmented interval, so at the end we got a number of values equal to the number of repetitions.

3 RESULTS

3.1 CoP parameters during unilateral stance

To analyze the parameters of the unilateral stance, the median of the three repetitions for each participant was considered. One of the two patients and one of the control participants did not perform this exercise.

We first compared the patient's results with those of the control group and then, within the control group, we analyzed the difference between the unilateral stance on the dominant and non-dominant side, and then in the lymphedema group the difference between the unilateral stance on the contralateral side.

3.1.1 Comparison between control group and lymphedema group

The results are shown in Figure 3.1. The distribution of the control group values was represented by box plots for both the unilateral stance on the leg of the dominant side (D) and of the non-dominant side (ND). Then the patient's values on both the lymphedema (L) and non-lymphedema (NL) side were compared with the normal ranges of the control group.

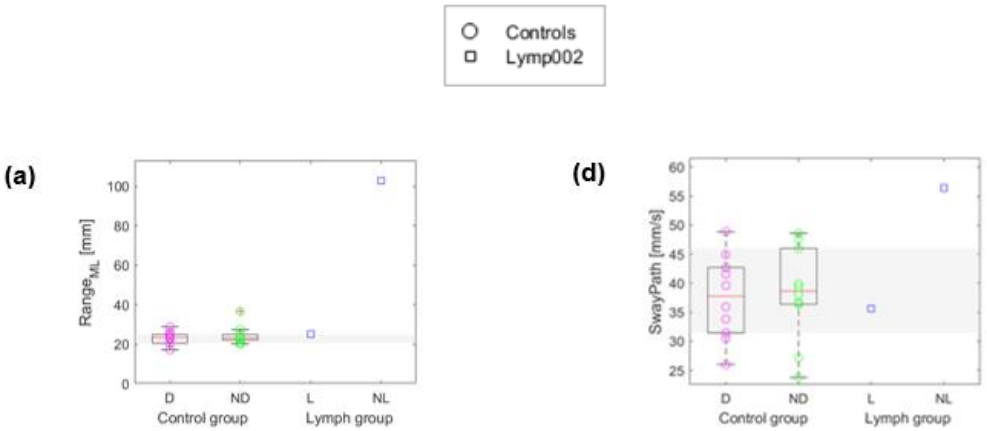

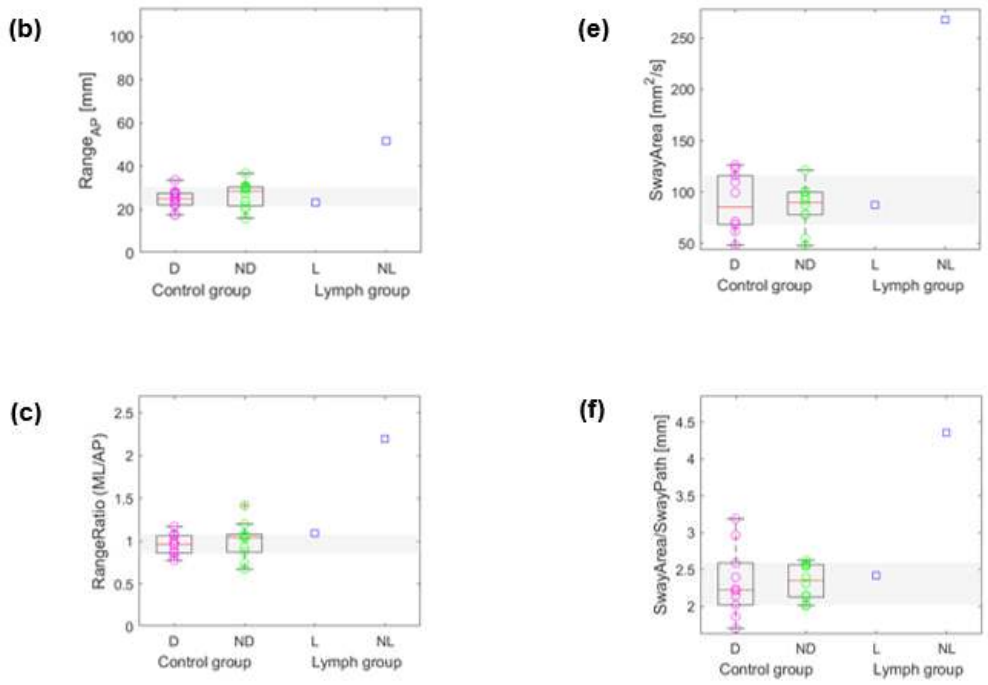

Figure 3.1 Unilateral stance parameters results: (a) $Range_{ML}$, (b)$Range_{AP}$, (c) $RangeRatio$, (d) $SwayPath$, (e) $SwayArea$, (f) $SwayArea/SwayPath$. The values of the control group are represented by box plot: the red line is the median value, the edges of the box are the 25th and 75th percentiles, the red crosses are the outliers. The circles are individual control values, the squares are Lymp002 patient values. The gray band represents the normal range of the control group. D = foot support on the dominant side, ND = foot support on the non-dominant side, L = foot support on the lymphedema side, NL = foot support on the side without lymphedema.

For all parameters the patient is outside the control ranges when performing the unilateral stance on the side without lymphedema. Instead, the values are within the control range when she is in unilateral stance on the side with lymphedema, except for $Range_{ML}$ where the value is at the upper limit of the range, and consequently also for $RangeRatio$.

3.1.2 Comparison between unilateral stance on the dominant and non-dominant side

To compare within each group the performance of the exercise standing first on one side and then on the other, we calculated for each participant in the control group the difference between standing on the dominant and non-dominant side (Δ D-ND), and for the patient the difference between standing on the side with lymphedema and without lymphedema (Δ L-NL). The distribution of the values for the control group was represented as a box plot (Figure 3.2).

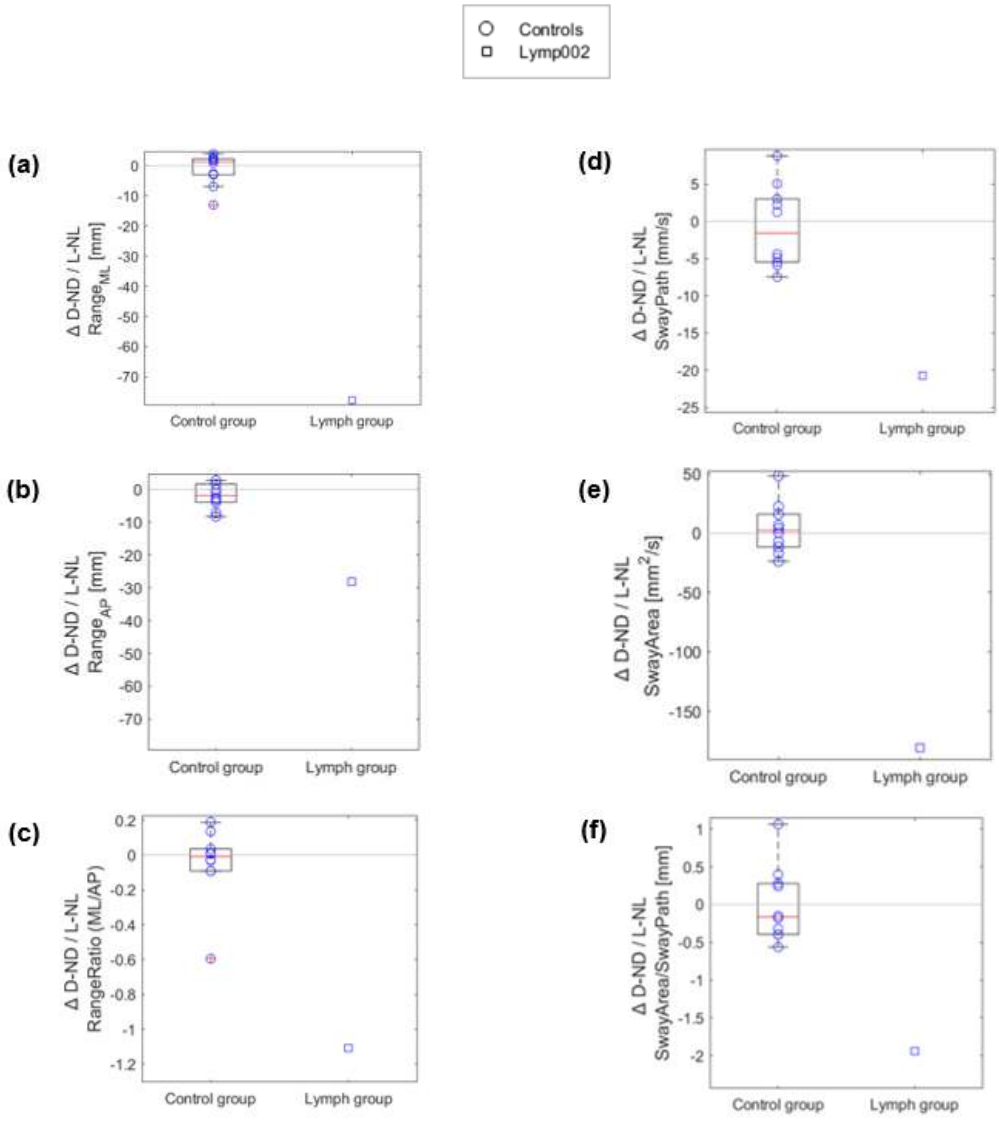

Figure 3.2 Differences between dominant and non-dominant side (ΔD-ND control group) and between side with lymphedema and without lymphedema (ΔL-NL lymphedema group) during unilateral stance: (a) $Range_{ML}$, (b)$Range_{AP}$, (c) $RangeRatio$, (d) $SwayPath$, (e) $SwayArea$, (f) $SwayArea/SwayPath$. The values of the control group are represented by box plot: the red line is the median value, the edges of the box are the 25th and 75th percentiles, the red crosses are the outliers. The circles are individual control values, the squares are Lymp002 patient values. D = foot support on the dominant side, ND = foot support on the non-dominant side, L = foot support on the lymphedema side, NL = foot support on the side without lymphedema.

In the control group, the differences between stance on the dominant and non-dominant side vary greatly from participant to participant for all parameters: some participants have a positive difference and others a negative difference, i.e., some have higher values on the dominant side while others on the non-dominant side. Instead, the patient always has a much greater difference compared to the control group, i.e., all parameters have higher values when standing on the side without lymphedema compared to the side with lymphedema.

3.2 CoP parameters during bilateral stance

For the calculation of the bilateral stance parameters, the time interval of interest was considered to be between 10 and 50 seconds in order not to include any oscillations in the initial and final phases of the recording.

We first compared the results of the lymphedema group with those of the control group and then, within each group, we analyzed the difference between bilateral stance with eyes closed and with eyes open.

3.2.1 Comparison between control group and lymphedema group

The results are shown in Figure 3.3. The distribution of the values of the control group was represented by box plots for both the bilateral stance with eyes open (EO) and with eyes closed (EC). The patient's values were then compared with the normal ranges of the control group.

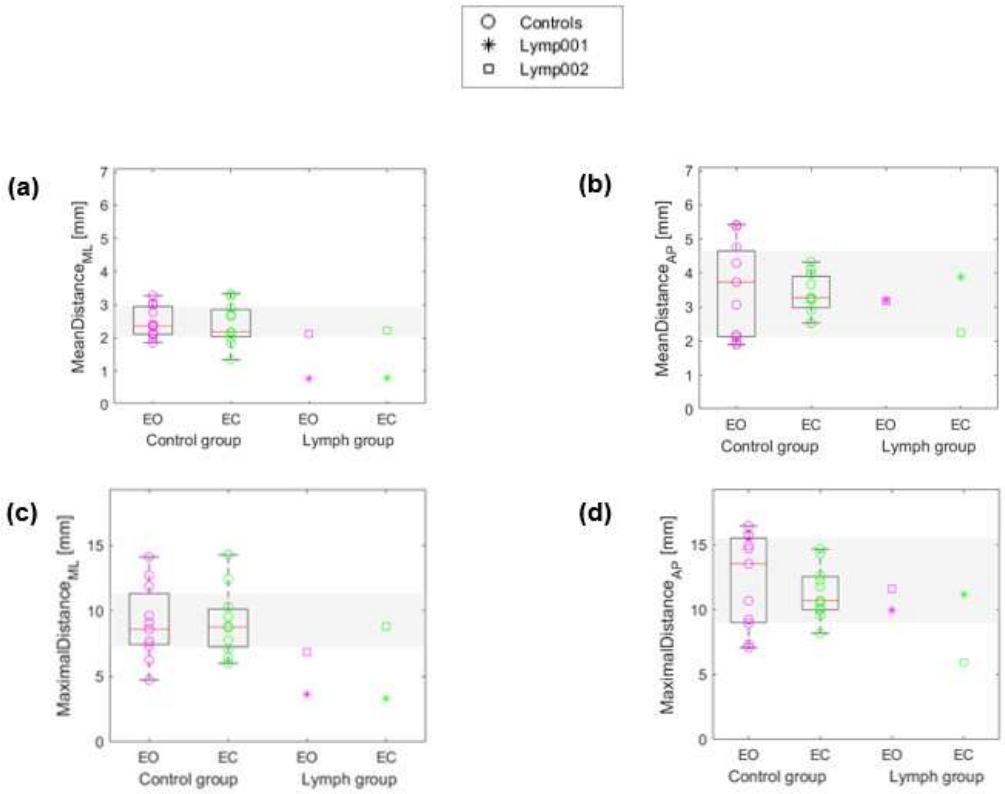

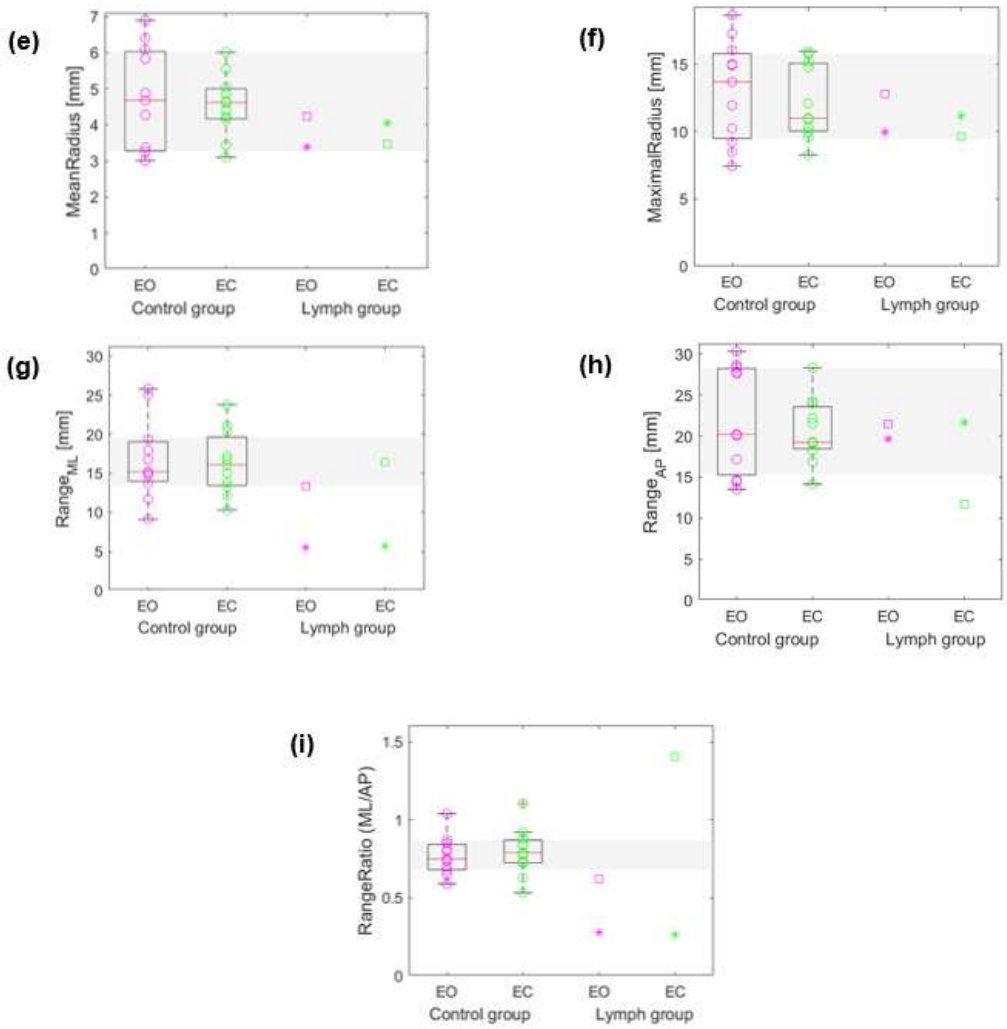

Figure 3.3 Bilateral stance parameters results: (a) $MeanDistance_{ML}$, (b) $MeanDistance_{AP}$, (c) $MaximalDistance_{ML}$, (d) $MaximalDistance_{ML}$, (e) $MeanRadius$, (f) $MaximalRadius$, (g) $Range_{ML}$, (h) $Range_{AP}$, (i) $RangeRatio$. The values of the control group are represented by box plot: the red line is the median value, the edges of the box are the 25th and 75th percentiles, the red crosses are the outliers. The circles are the values of the individual controls, the asterisks are the values of patient Lymp001, the squares are Lymp002 patient values. The gray band represents the normal range of the control group. EO = eyes open, EC = eyes closed.

In the control group $RangeRatio$ is on average less than 1, therefore the oscillations in ML direction are smaller than those in AP direction.

In all the parameters calculated along the ML direction ($MeanDistance_{ML}$, $MaximalDistance_{ML}$, $Range_{ML}$), the values of the patient Lymp001 are much lower than the corresponding control ranges, because she had her feet very far apart in the force platform during the acquisition, which leads to less oscillation in the ML direction. The patient Lymp002 has values below the control range for $Range_{AP}$ in the EC condition and slightly below the control range for $Range_{ML}$ in the EO condition.

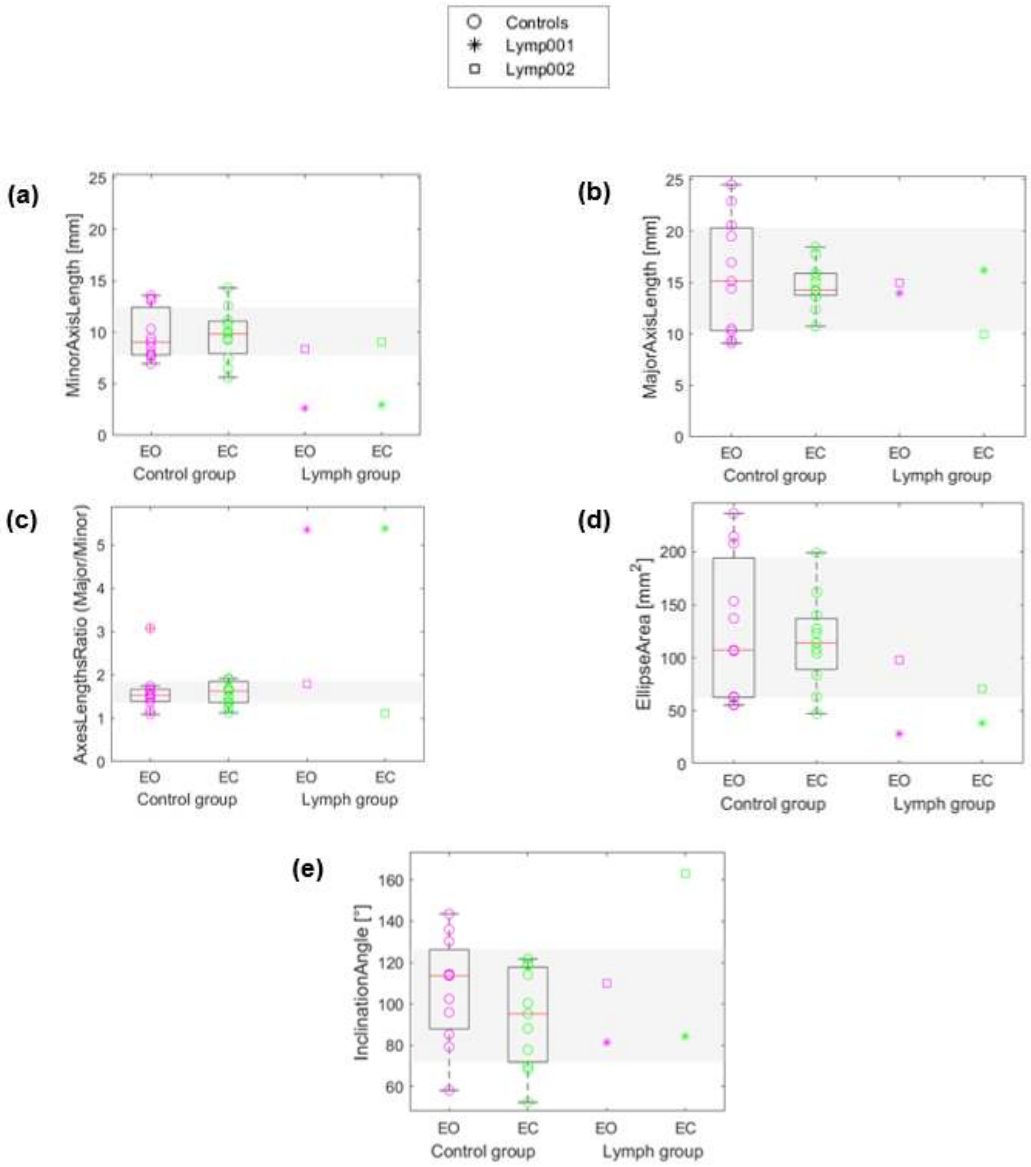

Figure 3.4 Bilateral stance parameters results: (a) $MinorAxisLength$, (b) $MajorAxisLength$, (c) $AxesLengthsRatio$, (d) $EllipseArea$, (e) $InclinationAngle$. The values of the control group are represented by box plot: the red line is the median value, the edges of the box are the 25th and 75th percentiles, the red crosses are the outliers. The circles are the values of the individual controls, the asterisks are the values of patient Lymp001, the squares are Lymp002 patient values. The gray band represents the normal range of the control group. EO = eyes open, EC = eyes closed.

The parameters calculated on the confidence ellipse are represented in Figure 3.4. $MinorAxisLength$ and $MajorAxisLength$ have values comparable respectively to $Range_{ML}$ and $Range_{AP}$ in both the control and lymphedema groups. The $InclinationAngle$ of the major axis with respect to x axis varies greatly from participant to participant. $EllipseArea$ in the patient Lymp001 has small values because she had her feet very far apart in the force platform during the acquisition, so the oscillations in the direction ML are very reduced and the ellipse takes a very flattened shape.

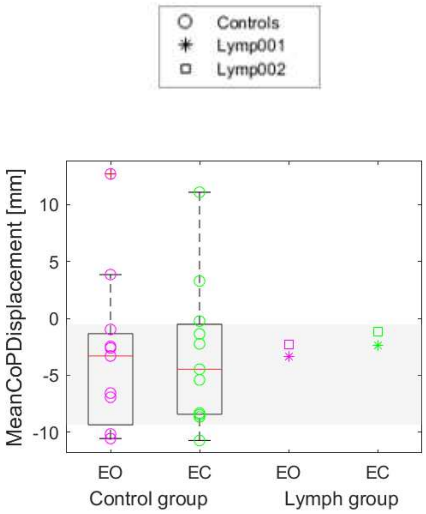

Figure 3.5 Bilateral stance parameters results: MeanCoPDisplacement. The values of the control group are represented by box plot: the red line is the median value, the edges of the box are the 25th and 75th percentiles, the red crosses are the outliers. The circles are the values of the individual controls, the asterisks are the values of patient Lymp001, the squares are Lymp002 patient values. The gray band represents the normal range of the control group. EO = eyes open, EC = eyes closed.

The distance between the average CoP and the straight line that passes through the central point between the heel markers and the central point between the second metatarsal markers is negative when it tends towards the non-dominant side (control group) or in the side where there is no lymphedema (lymphedema group). On average it is slightly negative in both groups. Patients have values close to the upper limit of the control range (see Figure 3.5).

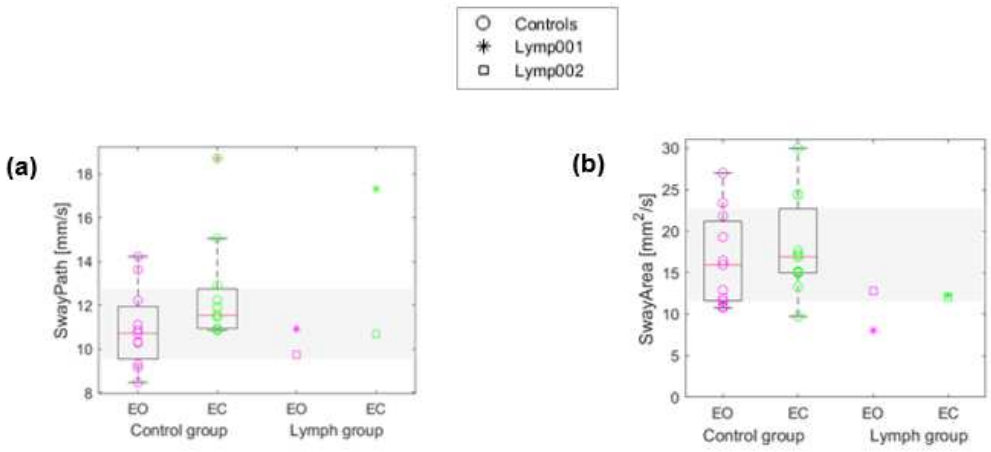

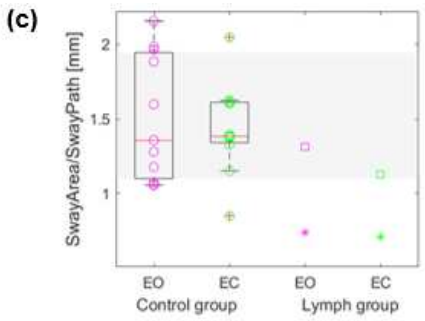

Figure 3.6 Bilateral stance parameters results: (a) $SwayPath$, (b) $SwayArea$, (c) $SwayArea/SwayPath$. The values of the control group are represented by box plot: the red line is the median value, the edges of the box are the 25th and 75th percentiles, the red crosses are the outliers. The circles are the values of the individual controls, the asterisks are the values of patient Lymp001, the squares are Lymp002 patient values. The gray band represents the normal range of the control group. EO = eyes open, EC = eyes closed.

The patient Lymp001 has smaller $SwayArea$ and also larger $SwayPath$ in EC compared to the control group, consequently $SwayArea/SwayPath$ ratio is lower than normal ranges (see Figure 3.6).

3.2.2 Comparison between eyes open and eyes closed conditions

To compare within each group the execution of the exercise with eyes closed and with eyes open, we calculated for each participant the difference between the values in the two conditions (Δ EC-EO). The distribution of the values of the control group was represented by a box plot. Results are shown in Figure 3.7, Figure 3.8, Figure 3.9, Figure 3.10.

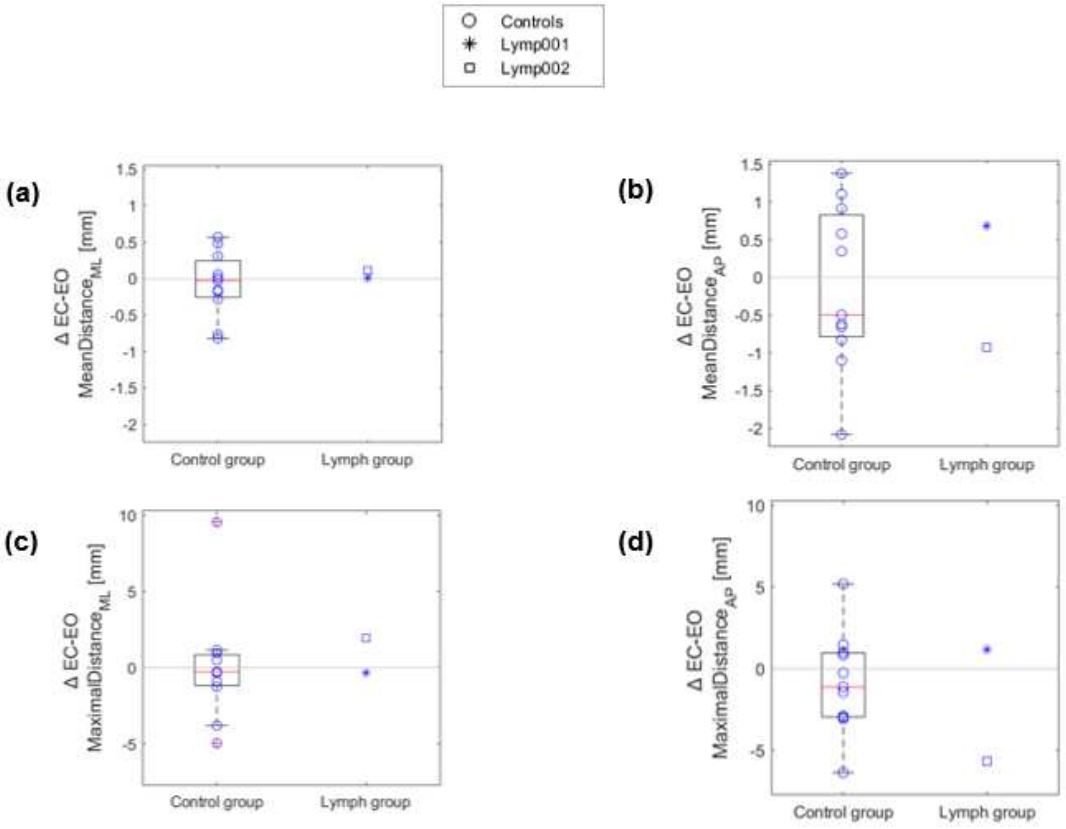

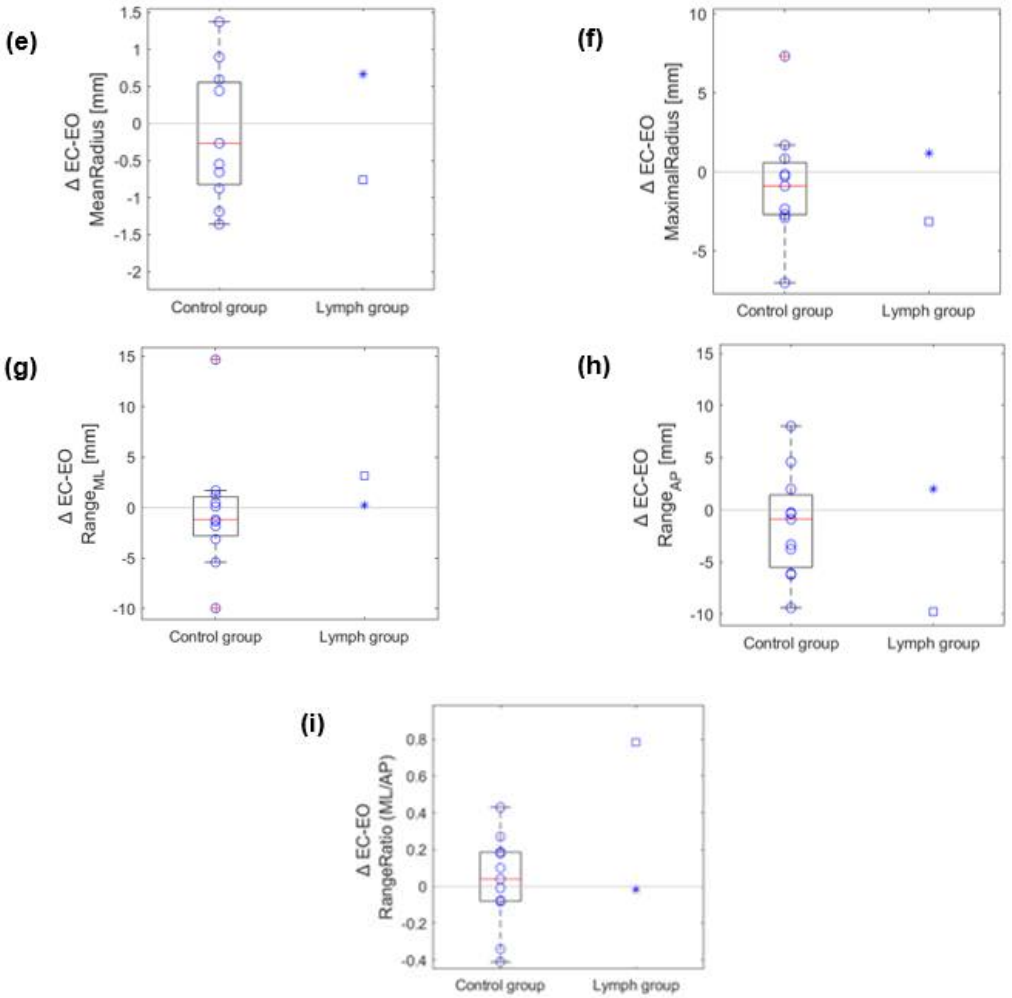

Figure 3.7 Differences between bilateral stance with eyes closed and eyes open (ΔEC-EO) during bilateral stance: (a) $MeanDistance_{ML}$, (b) $MeanDistance_{AP}$, (c) $MaximalDistance_{ML}$, (d) $MaximalDistance_{ML}$, (e) $MeanRadius$, (f) $MaximalRadius$, (g) $Range_{ML}$, (h) $Range_{AP}$, (i) $RangeRatio$. The values of the control group are represented by box plot: the red line is the median value, the edges of the box are the 25th and 75th percentiles, the red crosses are the outliers. The circles are the values of the individual controls, the asterisks are the values of patient Lymp001, the squares are Lymp002 patient values. EO = eyes open, EC = eyes closed.

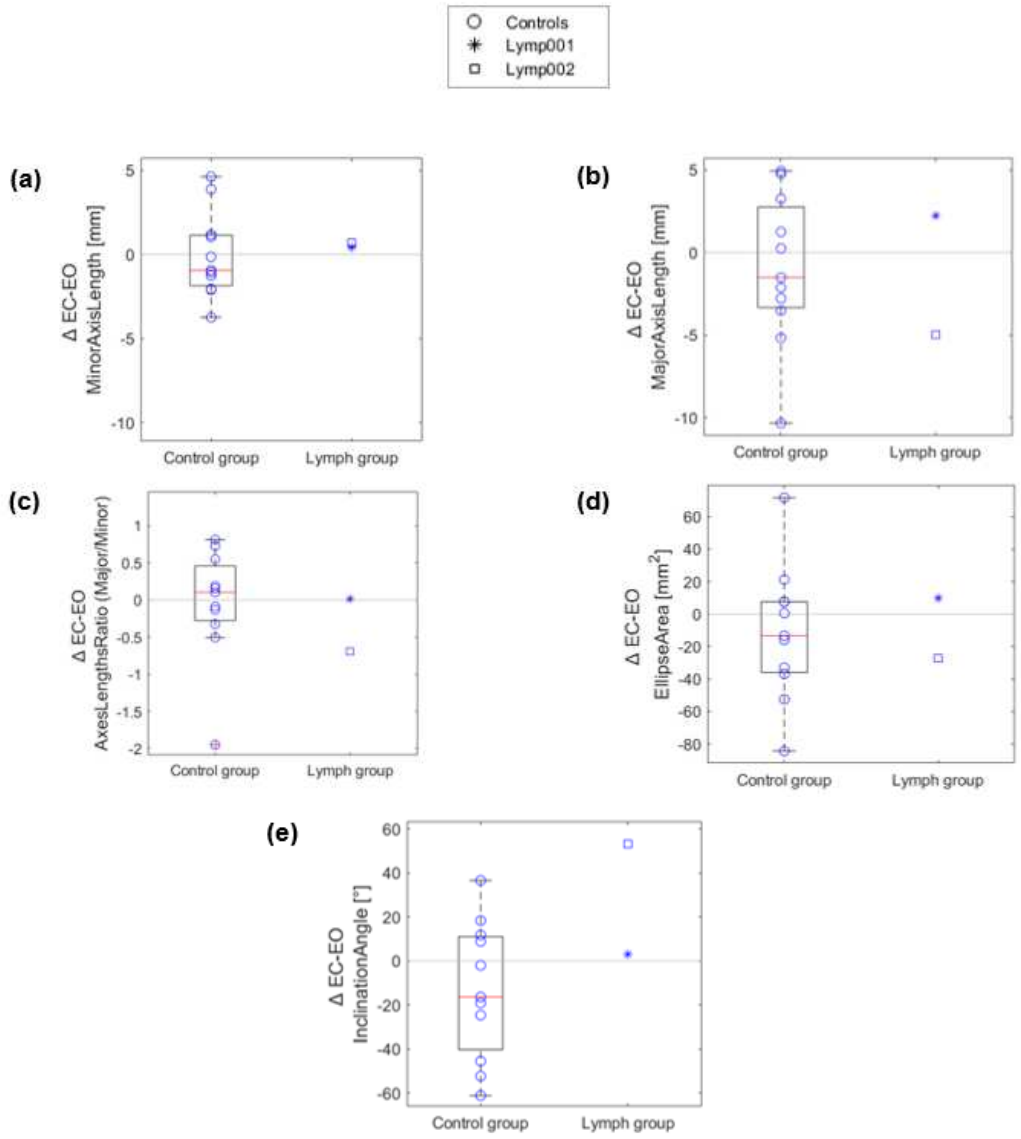

Figure 3.8 Differences between bilateral stance with eyes closed and eyes open (ΔEC-EO) during bilateral stance: (a) MinorAxisLength, (b) MajorAxisLength, (c) AxesLengthsRatio, (d) EllipseArea, (e) InclinationAngle. The values of the control group are represented by box plot: the red line is the median value, the edges of the box are the 25th and 75th percentiles, the red crosses are the outliers. The circles are the values of the individual controls, the asterisks are the values of patient Lymp001, the squares are Lymp002 patient values. EO = eyes open, EC = eyes closed.

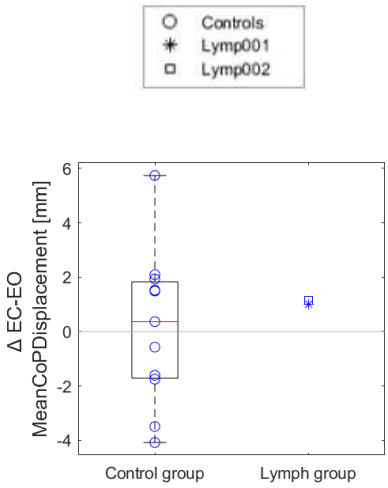

Figure 3.9 Differences between bilateral stance with eyes closed and eyes open (ΔEC-EO) during bilateral stance: MeanCoPDisplacement. The values of the control group are represented by box plot: the red line is the median value, the edges of the box are the 25th and 75th percentiles, the red crosses are the outliers. The circles are the values of the individual controls, the asterisks are the values of patient Lymp001, the squares are Lymp002 patient values. EO = eyes open, EC = eyes closed.

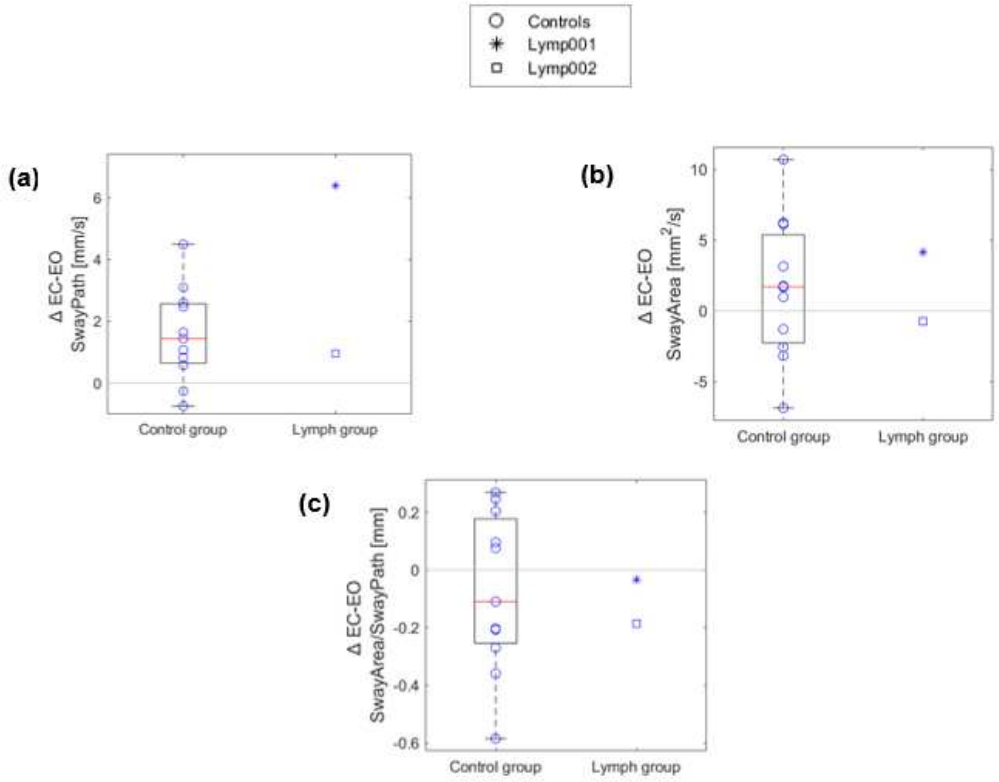

Figure 3.10 Differences between bilateral stance with eyes closed and eyes open (ΔEC-EO) during bilateral stance: (a) SwayPath, (b) SwayArea, (c) SwayArea/SwayPath. The values of the control group are represented by box plot: the red line is the median value, the edges of the box are the 25th and 75th percentiles, the red crosses are the outliers. The circles are the values of the individual controls, the asterisks are the values of patient Lymp001, the squares are Lymp002 patient values. EO = eyes open, EC = eyes closed.

In the control group the differences between EO and EC vary greatly from participant to participant in all parameters: some participants have a positive difference and others a negative one, i.e. some have higher values in EO while others in EC except for the $SwayPath$ parameter which for almost all participants has a positive difference so it is greater in EC. The patient Lymp001 is always close to the control range except in $SwayPath$ where it is much higher. The patient Lymp002 goes outside the control ranges in the parameters calculated in the two directions, in particular in EC she tends to decrease the oscillations in AP and slightly increase the oscillations in ML.
We compared the results between eyes open and eyes closed conditions performing a two-sided sign test. If we consider the significance level at 5%, no parameter revealed a significant difference between the two conditions but the parameter in which the p-value comes closest to the significance threshold is $SwayPath$ with a p-value of 0.06543.

3.3 CoP parameters during upper limb functional tasks

To analyze the parameters of the unilateral stance, the median of the three repetitions for each participant was considered.
We first compared the patient's results with those of the control group and then, within the control group, we analyzed the difference between exercises performed with the dominant and non-dominant arm, and then in the lymphedema group the difference between exercises performed with the arm with lymphedema and the contralateral one.
The results obtained from performing the task with both arms did not show any useful information to characterize postural control therefore we focused on tasks performed with a single arm.

3.3.1 Comparison between control group and lymphedema group

The distribution of the control group values was represented by box plots for both the tasks executed with the dominant arm (D) and with the non-dominant arm (ND). Then the patient's values on both lymphedema (L) and non-lymphedema (NL) side were compared with the normal ranges of the control group. The results are shown in Figure 3.11.

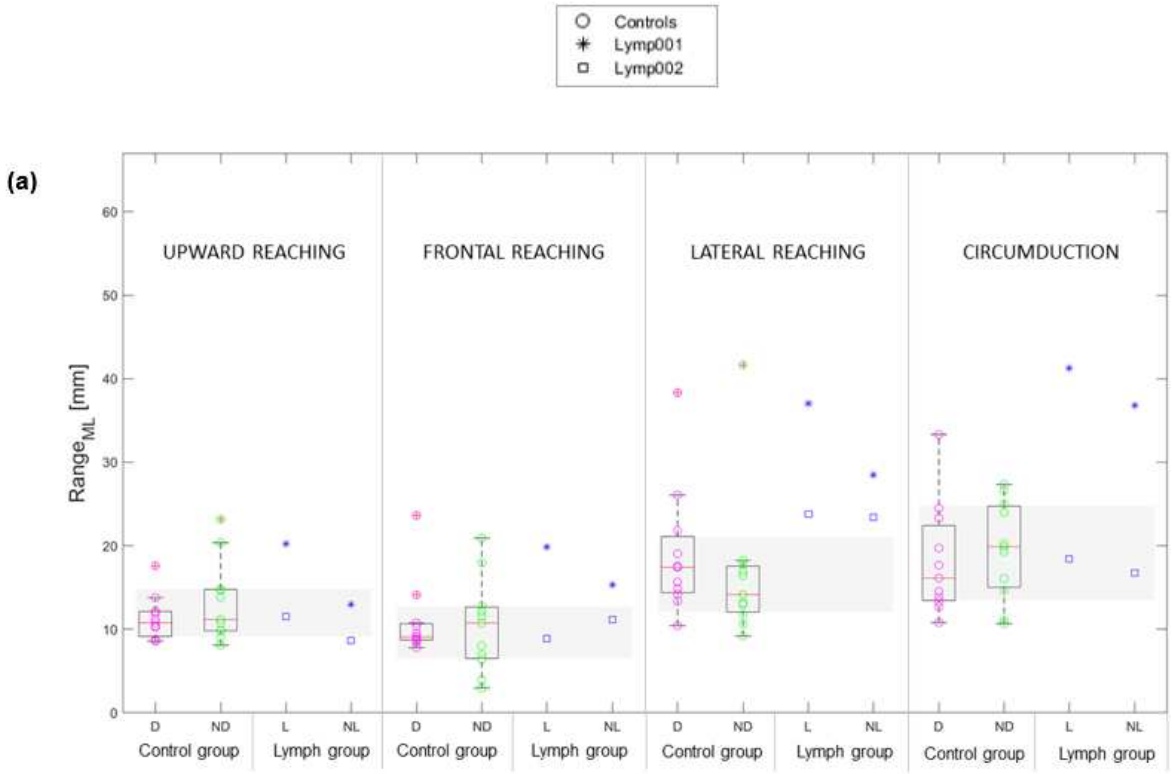
(a)
Controls
Lymp001
Lymp002
UPWARD REACHING
FRONTAL REACHING
LATERAL REACHING
CIRCUMDUCTION
Range_ML [mm]
0
10
20
30
40
50
60
D
ND
L
NL
Control group
Lymph group

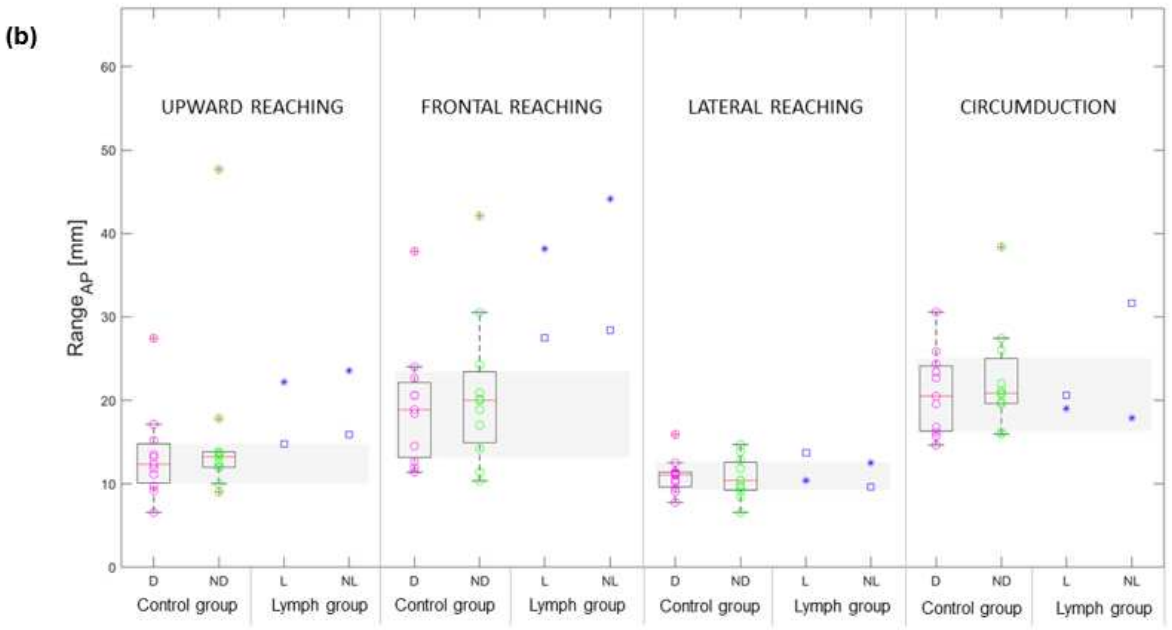
(b)
UPWARD REACHING
FRONTAL REACHING
LATERAL REACHING
CIRCUMDUCTION
Range_AP [mm]
0
10
20
30
40
50
60
D
ND
L
NL
Control group
Lymph group

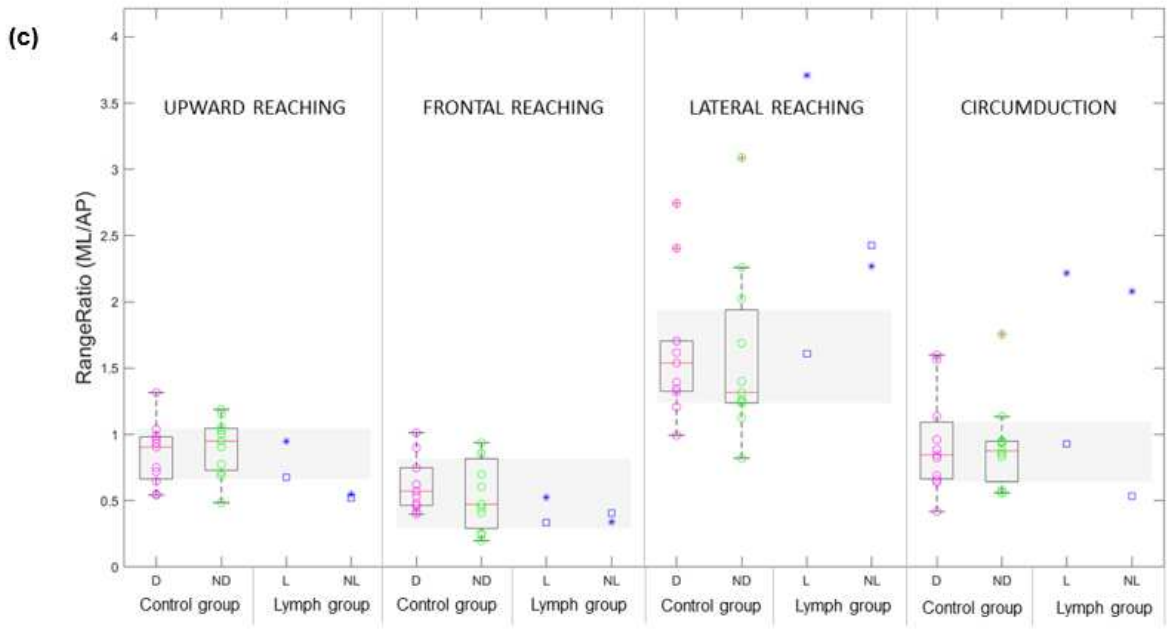

Figure 3.11 Upper limb functional tasks parameters results: (a) $Range_{ML}$, (b) $Range_{AP}$, (c) $RangeRatio$. The values of the control group are represented by box plot: the red line is the median value, the edges of the box are the 25th and 75th percentiles, the red crosses are the outliers. The circles are the values of the individual controls, the asterisks are the values of patient Lymp001, the squares are Lymp002 patient values. The gray band represents the normal range of the control group. D = movement performed with the dominant arm, ND = movement performed with the non-dominant arm, L = movement performed with the lymphedema arm, NL = movement performed with the arm without lymphedema.

Due to the nature of the exercises, while in upward reaching and circumduction $RangeRatio$ is around 1, the greatest difference between the oscillation ranges in the two directions occurs in lateral reaching, where the oscillations are greater in ML direction, and in frontal reaching, where the oscillations in AP direction are greater.

Comparing the control group and the lymphedema group, we note that the difference is evident especially in these last two exercises. In fact, they are the only ones in which both patients are outside the control range: for $Range_{ML}$ of lateral reaching and for $Range_{AP}$ of frontal reaching. The patient Lymp001 is out of range also in the other exercises, especially in the $Range_{ML}$ parameter.

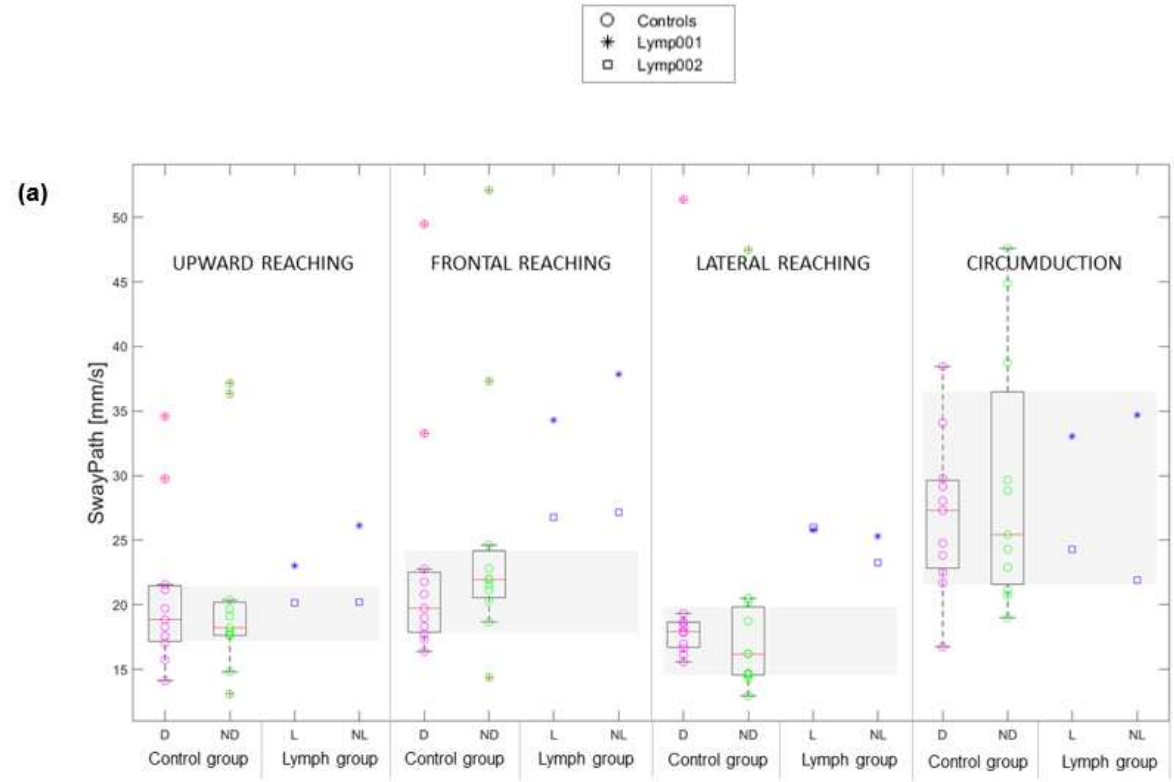
Controls
Lymp001
Lymp002
(a)
UPWARD REACHING
FRONTAL REACHING
LATERAL REACHING
CIRCUMDUCTION
SwayPath [mm/s]
D
ND
L
NL
Control group
Lymph group

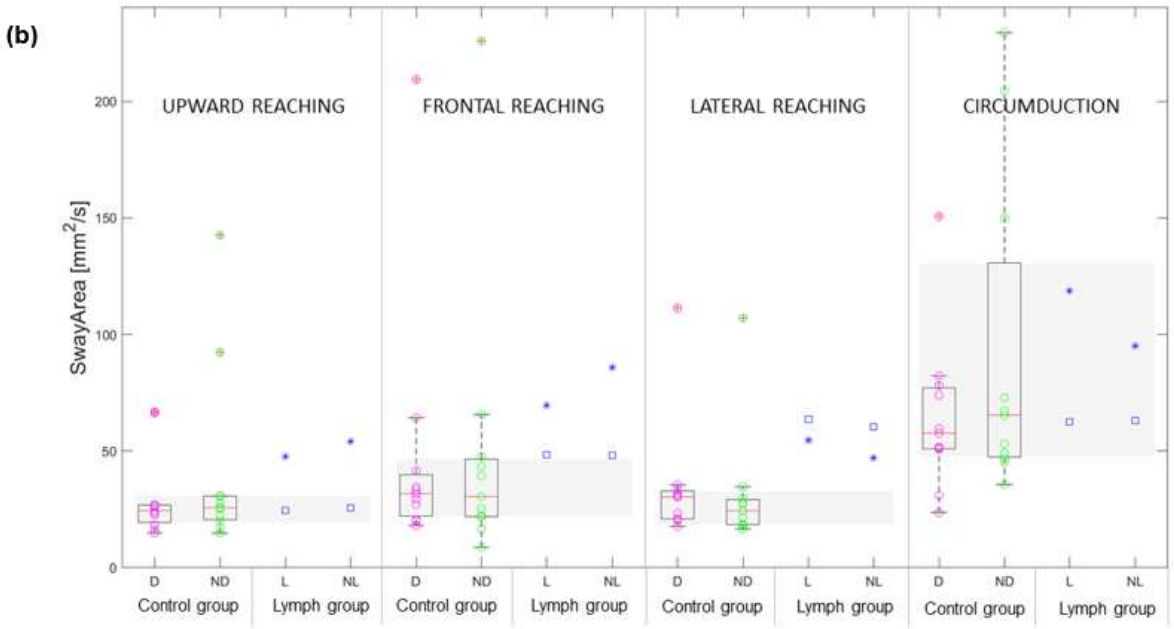
(b)
UPWARD REACHING
FRONTAL REACHING
LATERAL REACHING
CIRCUMDUCTION
SwayArea [mm²/s]
D
ND
L
NL
Control group
Lymph group

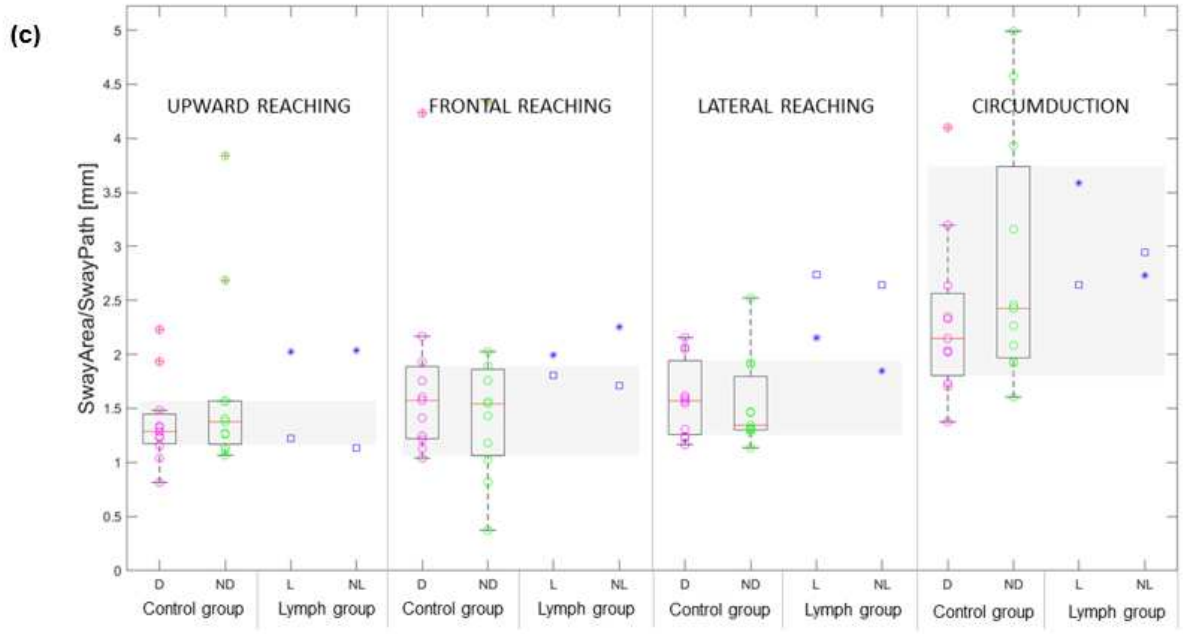

Figure 3.12 Upper limb functional tasks parameters results: (a) SwayPath, (b) SwayArea, (c) SwayArea/SwayPath. The values of the control group are represented by box plot: the red line is the median value, the edges of the box are the 25th and 75th percentiles, the red crosses are the outliers. The circles are the values of the individual controls, the asterisks are the values of patient Lymp001, the squares are Lymp002 patient values. The gray band represents the normal range of the control group. D = movement performed with the dominant arm, ND = movement performed with the non-dominant arm, L = movement performed with the lymphedema arm, NL = movement performed with the arm without lymphedema.

The results of dynamic parameters are shown in Figure 3.12. Both patients are outside the control ranges of both $SwayPath$ and $SwayArea$ in frontal reaching and lateral reaching. The patient Lymp001 is also out of range in upward reaching.

3.3.2 Comparison between tasks executed with the dominant and non-dominant arm

To compare within each group the performance of the exercises executed with one arm and then with the other one, we calculated for each participant in the control group the difference between task executed with the dominant and non-dominant side (Δ D-ND), while for the patient the difference between task executed on the side with lymphedema and without lymphedema (Δ L-NL). The distribution of the values for the control group was represented as a box plot. The results are shown in Figure 3.13 and Figure 3.14.

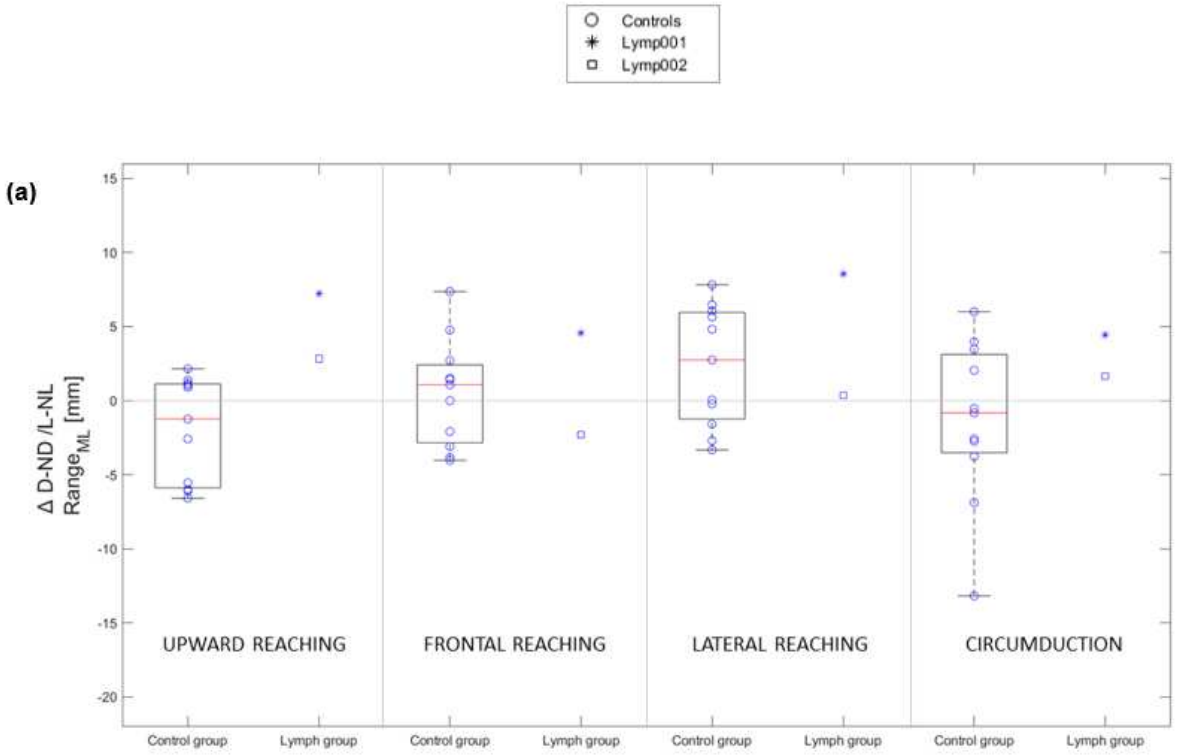
Controls
Lymp001
Lymp002
(a)
Δ D-ND /L-NL
Range_ML [mm]
15
10
5
0
-5
-10
-15
-20
UPWARD REACHING
FRONTAL REACHING
LATERAL REACHING
CIRCUMDUCTION
Control group
Lymph group
Control group
Lymph group
Control group
Lymph group
Control group
Lymph group

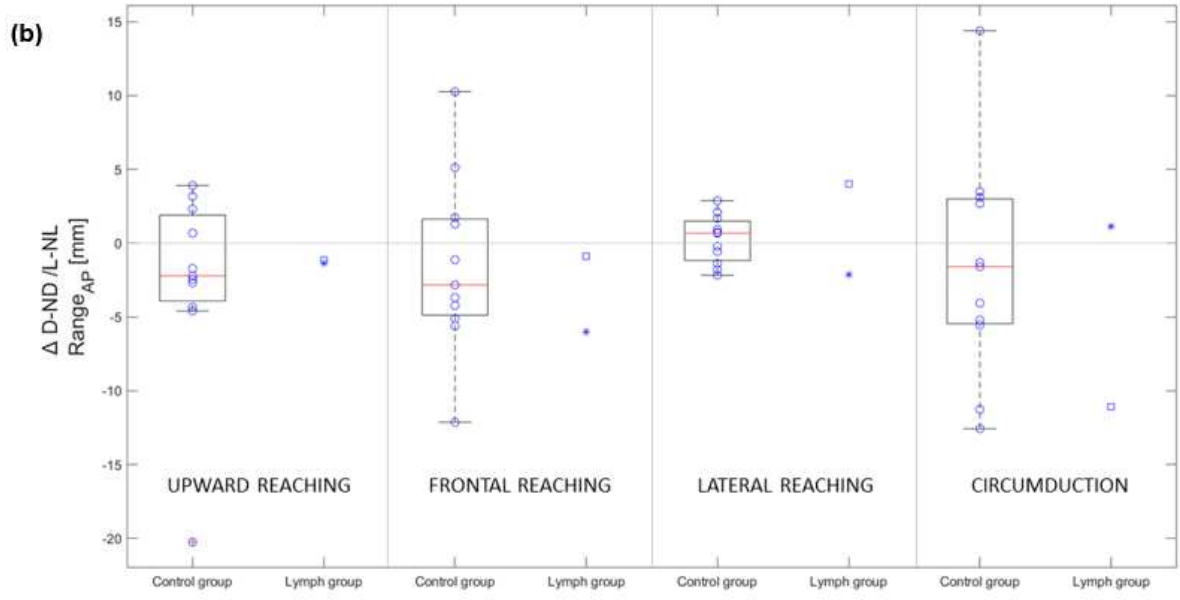
(b)
Δ D-ND /L-NL
Range_AP [mm]
15
10
5
0
-5
-10
-15
-20
UPWARD REACHING
FRONTAL REACHING
LATERAL REACHING
CIRCUMDUCTION
Control group
Lymph group
Control group
Lymph group
Control group
Lymph group
Control group
Lymph group

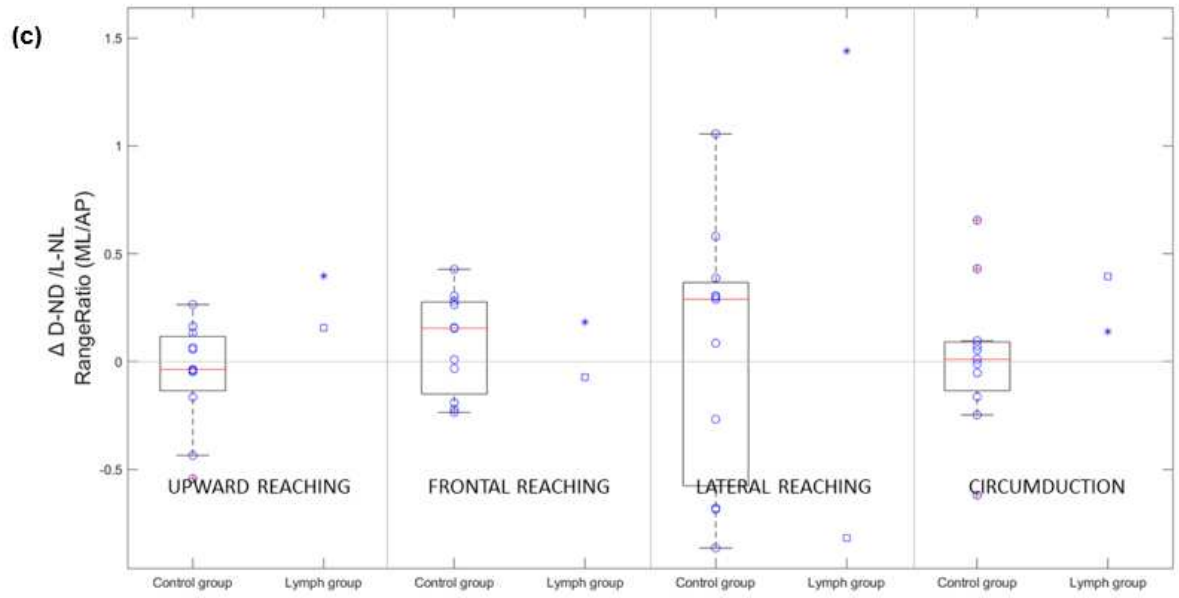

Figure 3.13 Differences between dominant and non-dominant side (ΔD-ND control group) and between side with lymphedema and without lymphedema (ΔL-NL lymphedema group) during upper limb functional tasks: (a) $Range_{ML}$, (b) $Range_{AP}$, (c) $RangeRatio$. The values of the control group are represented by box plot: the red line is the median value, the edges of the box are the 25th and 75th percentiles, the red crosses are the outliers. The circles are the values of the individual controls, the asterisks are the values of patient Lymp001, the squares are Lymp002 patient values. D = movement performed with the dominant arm, ND = movement performed with the non-dominant arm, L = movement performed with the lymphedema arm, NL = movement performed with the arm without lymphedema.

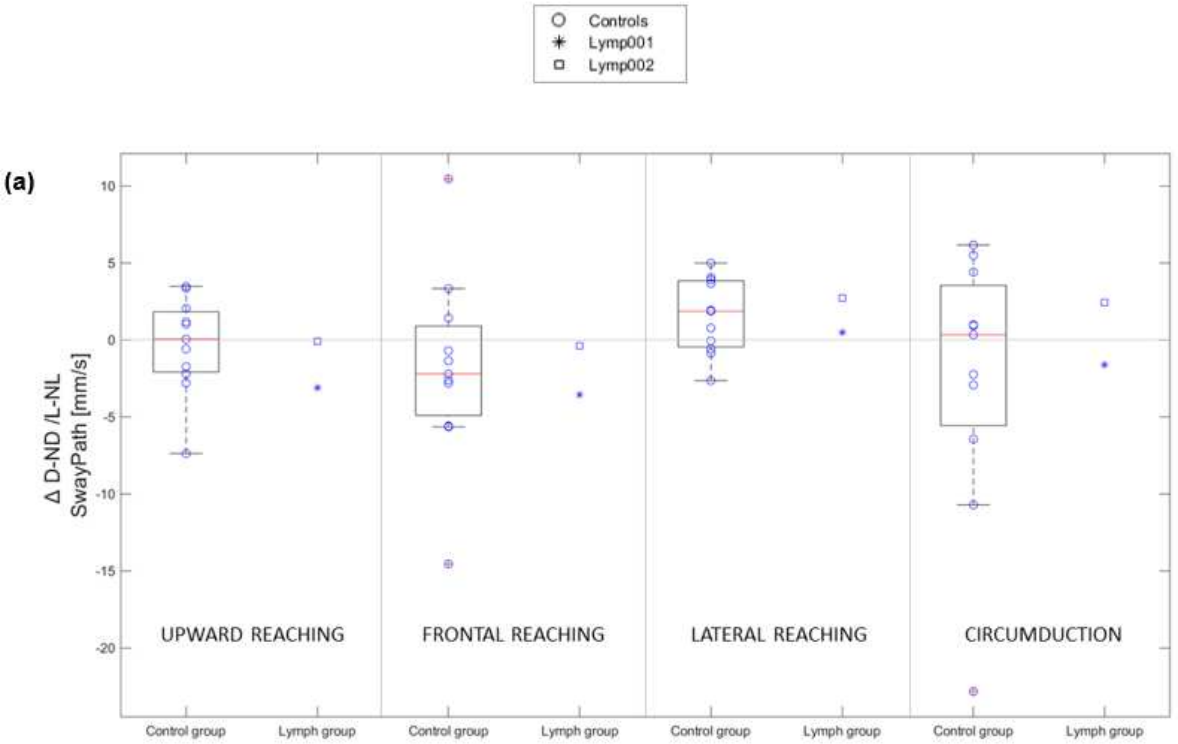
Controls
Lymp001
Lymp002
(a)
Δ D-ND /L-NL SwayPath [mm/s]
10
5
0
-5
-10
-15
-20
UPWARD REACHING
FRONTAL REACHING
LATERAL REACHING
CIRCUMDUCTION
Control group
Lymph group

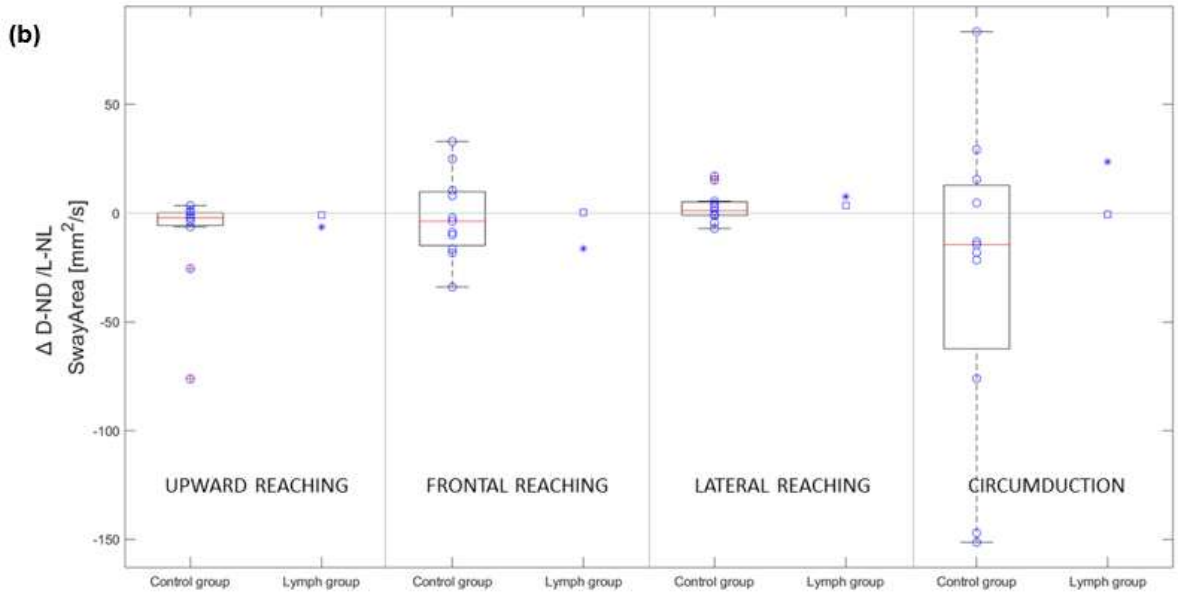
(b)
Δ D-ND /L-NL SwayArea [mm²/s]
50
0
-50
-100
-150
UPWARD REACHING
FRONTAL REACHING
LATERAL REACHING
CIRCUMDUCTION
Control group
Lymph group

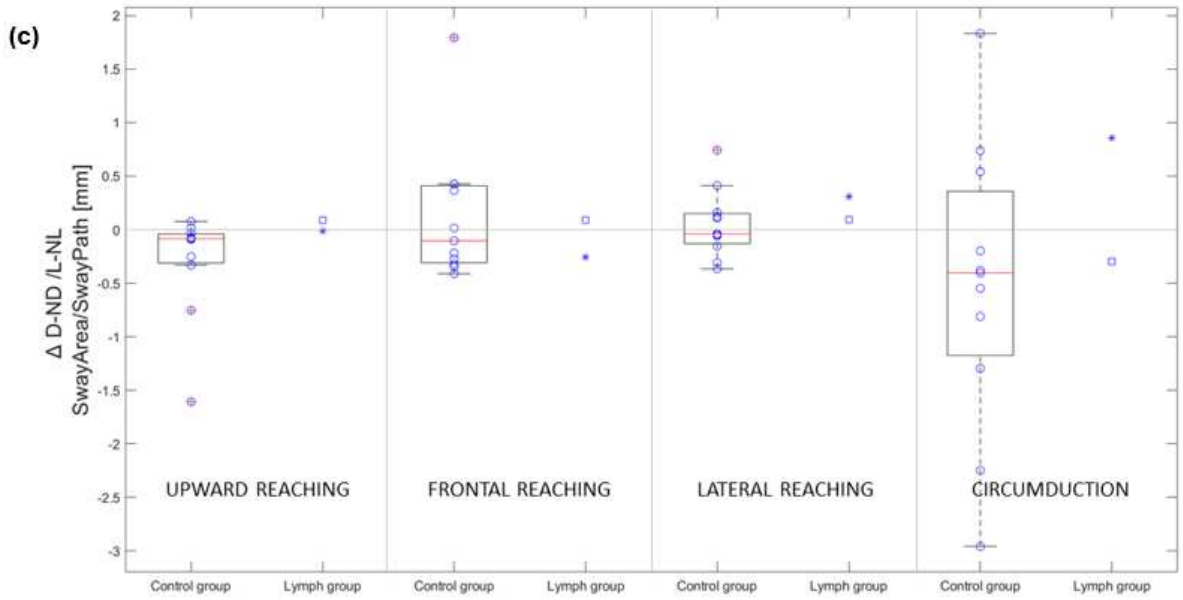

Figure 3.14 Differences between dominant and non-dominant side (ΔD-ND control group) and between side with lymphedema and without lymphedema (ΔL-NL lymphedema group) during upper limb functional tasks: (a) $SwayPath$, (b) $SwayArea$, (c) $SwayArea/SwayPath$. The values of the control group are represented by box plot: the red line is the median value, the edges of the box are the 25th and 75th percentiles, the red crosses are the outliers. The circles are the values of the individual controls, the asterisks are the values of patient Lymp001, the squares are Lymp002 patient values. D = movement performed with the dominant arm, ND = movement performed with the non-dominant arm, L = movement performed with the lymphedema arm, NL = movement performed with the arm without lymphedema.

In the control group, the differences between D and ND arm vary greatly from participant to participant in all parameters: some participants have a positive difference and others a negative difference, i.e., some have higher values on the dominant side while others on the non-dominant side.

In $Range_{AP}$, $SwayPath$ and $SwayArea$ the patients almost always have values close to the control ranges while in $Range_{ML}$ Lymp001 is outside in all exercises, in particular it has much greater oscillations when it performs movements with the arm with lymphedema.

4 DISCUSSION

The predominant CoP oscillation in bilateral stance is antero-posterior, which is why the confidence ellipse has an elongated rather than wide shape in the majority of cases. In fact, the results of the control group show that the parameters calculated along the ML direction have smaller values on average compared to the AP direction. Similar results were found in the review by Quijoux et al. [13]. Instead, when balancing on one foot, the area over which the weight is distributed is reduced to the sole of the supported foot which, being longer than wide, leads to an increase in oscillations in the medio-lateral direction. When performing movements with the arms, the trajectory of the CoP varies according to the predominant direction in which the movement is performed, therefore the results must be interpreted taking into account the nature of the exercises: in lateral reaching, there are greater oscillations along the medio-lateral direction, in frontal reaching along the antero-posterior direction, in upward reaching and in circumduction neither of the two directions is predominant.

Within the control group, none of the calculated parameters highlights a different postural strategy between the dominant and non-dominant side, neither in the unilateral stance test nor in the exercises performed with one arm. Regarding the unilateral stance, if we look at the differences in the parameters calculated in the control group between the two sides, we notice that they vary greatly from participant to participant: some have greater CoP oscillations, speed and areas when performing the exercise on the dominant side and others on the non-dominant side. This variability is consistent with what was found in the study by Paillard et al. [19] which analyzed the difference in postural control between the two legs during single-leg balance. Typically, the dominant leg performs a motor task requiring strength and accuracy while the non-dominant leg supports body mass. This might suggest greater stability in the non-dominant leg, but there are several factors that influence the relationship between limb dominance and postural balance. These factors can be intrinsic, such as morphology, muscle strength, proprioception, hemispheric laterality, but also, for example, the physical activity performed can lead to postural adaptations if only the limb on one side is specialized. If we consider a population that does not perform highly specialized motor tasks with one leg compared to the other, there are no differences in balance between the two legs. These considerations lead to the conclusion that the influence of limb dominance on monopodal postural balance is likely to be

context dependent, and that the leg showing better postural performance can be either the dominant or non-dominant leg [19].

With regard to the functional tasks of the upper limb, the comparison between the performance of the task with one arm and the other was found to be vary variable among the participants, with some having greater CoP oscillations, speeds and areas when performing the task with the dominant limb and others with the non-dominant limb.

Regarding the comparison between balance with eyes open and with eyes closed, the only parameter that was found to be discriminative in both the control and lymphedema groups was the sway path. In fact, almost all participants have a greater CoP oscillation speed when they perform the exercise with their eyes closed. This difference is accentuated in one of the two patients with lymphedema. Similar results were found by Angin et al. [4], Hsieh et al. [5], Schimmel et al. [20] and Chiari et al. [21]. Vision is important for body stabilization during standing, in fact, when it is available, participants reduce reliance on proprioception and increase reliance on the visual system. Vision provides visual information about our surrounding environment, contributes to our sense of orientation and balance, and it is able to gate the effects of muscle vibrations that would cause oscillations of the CoP [22]. When the eyes are closed, the oscillation speed of the CoP increases, participants can no longer rely on visual information and therefore rely more on proprioception. Proprioception plays a critical role in postural control by providing information about the position of body parts in space, in order to activate appropriate muscle responses to counteract destabilizing forces and keep the center of mass stable [5]. The loss of proprioception that often occurs after cancer treatment may be the cause of the increase in the CoP sway speed in patients compared to the controls in situations where visual feedback is lacking. Therefore, the results suggest that breast cancer survivors have impaired balance when compared to normative values of adults who have never had breast cancer because they rely heavily on visual feedback to maintain upright posture [5].

Comparing the results of the patients with those of the control group, it was observed that the presence of lymphedema influences the trajectory of the CoP. In particular, the patient who performed unilateral stance goes outside the normal ranges of both position and dynamic parameters when balancing on the side without lymphedema. A similar result was obtained by Angin et al. [4], who studied the postural sway speed during unilateral stance in patients with lymphedema and found that it was even higher on the contralateral side when compared to the ipsilateral side. These findings may indicate that controlling the position of the CoP became difficult because the distance from the local center of gravity of the upper limb with lymphedema to the contralateral supporting lower limb was greater than the distance to the ipsilateral side.

The parameters calculated during the bilateral balance of the same patient did not highlight values outside the control range, therefore it can be assumed that the unilateral stance has greater discriminatory power than the bilateral stance. Furthermore, in the bilateral stance the positioning of the feet on the force platform could influence the stability of the participant; in fact, the further the feet are far from each other, the less the oscillations in the medio-lateral direction are and, therefore, the narrower the confidence ellipse is. This is the case for one of the two patients in the lymphedema group, who kept her feet far apart during the bilateral stance tests due to balance problems caused by her weight.

If we consider the position of the CoP midpoint with respect to an axis of symmetry, which we have defined as the straight line passing through the midpoint between the heel markers and the midpoint between the second metatarsal markers, the CoP of the patients is shifted more toward the side affected by the lymphedema compared to the average position of the control group. In fact, the lymphedema swelling can be considered as a unilateral weight bearing in the upright position which shifts the body weight toward the load and the CoP is shifted to the ipsilateral side of the load [4].

Regarding the arm movement exercises, two of them seem to have a greater discriminatory power between the two groups: lateral reaching and frontal reaching. In fact, both patients are outside the normal ranges in some parameters of these exercises: the range of oscillation in the medio-lateral direction in lateral reaching, the range of oscillation in the antero-posterior direction in frontal reaching, both the sway path and the sway area in both exercises. Only one of the two patients is outside the control range even in the medio-lateral oscillations when she performs the movement with the ipsilateral arm in all exercises. A larger number of samples could help to obtain statistically significant results.

5 CONCLUSION

In this thesis, we analyzed postural control during upper limb functional tasks while standing exploiting the center of pressure signal. A group of eleven healthy women and two patients with lymphedema participated in this study and were asked to perform a series of tasks in an environment equipped with an optoelectronic system and a force platform. Since several repetitions were performed for each task, an algorithm was developed to identify the start and end moments of the movement. It is based on the analysis of the position and speed distribution of the markers placed on the participant's body, specifically those placed on the elbows, in the case of the upper limb functional task, and on the heel of the lifted foot, in the case of the unilateral stance. By analyzing the trend of the histogram of the root mean square logarithm of both position and speed, the algorithm automatically identifies the threshold that distinguishes movement from rest in each task. The algorithm performs well if the participant stands in neutral position for at least a couple of seconds between repetitions. If this does not happen there may not be the recurring trend of the histogram so the identified threshold may not segment the movement well. A future development could be to study this case and find ways to make the analysis independent of the time spent between one repetition and another. After identifying the intervals of interest for the CoP analysis we moved on to the calculation of parameters that define the main characteristics of the CoP trajectory. We analyzed balance maintenance during the standing position in bilateral stance, and we studied how the oscillations vary during unilateral stance or when performing exercises with arm movements. Some of these have proven to be more effective in evaluating a different postural control strategy between controls and patients with lymphedema. In particular, due to the increased volume in the arm with lymphedema, when the patient performed the unilateral stance with the contralateral leg, she went out of the normal range in all parameters, in contrast to the bilateral stance in which there was no sign of difference with the control group. Regarding the exercises with arm movements, the most discriminatory ones seem to be the frontal reaching and lateral reaching, since these are the exercises in which both patients are outside the normal ranges in the parameters of sway path, sway area and the oscillation range in the predominant direction of movement of the arms. A larger number of samples will allow the evaluation of statistically significant differences. Furthermore, the sway path proved to be the most effective parameter

to discriminate between the open-eye and closed-eye bilateral stance, in fact in the absence of visual information the speed of the CoP increases. In the case of a patient with lymphedema, since the worsening of proprioception is a possible consequence of cancer treatment, this comparison can be useful to define the effectiveness of a therapy.

Bibliography

[1] Maccarone M, Venturini E, Menegatti E, Gianesini S, Masiero S, "Water-based exercise for upper and lower limb lymphedema treatment," *Journal of Vascular Surgery: Venous and Lymphatic Disorders,* vol. 11, no. 1, pp. 201-209, 2023.

[2] International Society of Lymphology, "The diagnosis and treatment of peripheral lymphedema: 2020 consensus document of the International Society of Lymphology," vol. 53, pp. 3-19, 2020.

[3] URL: https://www.sigvaris.com.

[4] Angin S, Karadibak D, Yavuzşen T, Demirbüken İ, "Unilateral upper extremity lymphedema deteriorates the postural stability in breast cancer survivors," Contemp Oncol (Pozn), 2014.

[5] Hsieh K, BS a, Wood T, An R, Trinh L, Sosnoff J, "Gait and Balance Impairments in Breast Cancer Survivors: A Systematic Review and Meta-analysis of Observational Studies," *Archives of Rehabilitation Research and Clinical Translation,* vol. 1, no. 1-2, 2019.

[6] Foley M P, Hasson S M, "Effect of a Community-Based Multimodal Exercise Program on Health-Related Physical Fitness and Physical Function in Breast Cancer Survivors: A Pilot Study," *Integrative Cancer Therapies,* vol. 15, no. 4, pp. 446-454, 2016.

[7] Kneis S, Wehrle A, Freyler K, Lehmann K, Rudolphi B, Hildenbrand B, Bartsch H H, Bertz H H, Gollhofer A, Ritzmann R, "Balance impairments and neuromuscular changes in breast cancer patients with chemotherapy-induced peripheral neuropathy," *Clinical Neurophysiology,* vol. 127, pp. 1481-1490, 2016.

[8] Monfort S M, Pan X, Patrick R, Singaravelu J, Loprinzi C L, Lustberg M B, ChaudHari A M W, "Natural history of postural instability in breast cancer patients treated with taxane-based chemotherapy: A pilot study," *Gait & Posture,* vol. 48, pp. 237-242, 2016.

[9] Wampler M A, Topp K S, Miaskowsky C, Byl N N, Rugo H S, Hamel K, "Quantitative and Clinical Description of Postural Instability in Women With Breast Cancer Treated With Taxane Chemotherapy," *Arch Phys Med Rehabil,* vol. 88, 2007.

[10] Montezuma T, Guirro E C, Vaz M M, Vernal S, "Changes in Postural Control in Mastectomized Women," *Journal of Cancer Therapy,* vol. 5, pp. 493-499, 2014.

[11] Basar S, Bakar Y, Keser I, Kaba H, Güzel N A, Özdemir O C, Düzgün I, "Does Lymphedema Affect the Postural Stability in Women After Breast Cancer?," *Geriatric Rehabilitation,* vol. 28, no. 4, pp. 1-8, 2012.

[12] Prieto T E, Myklebust J B, Hoffmann R G, "Measures of postural steadiness: differences between healthy young and elderly adults," *IEEE TRANSACTIONS ON BIOMEDICAL ENGINEERING,* vol. 43, no. 9, pp. 956-966, 1996.

[13] Quijoux F, Nicolaï A, Chairi I, Bargiotas I, Ricard D, Yelnik A, Oudre L, Bertin-Hugault F, Vidal P, Vayatis N, Buffat S, Audiffren J, "A review of center of pressure (COP) variables to quantify standing balance in elderly people: Algorithms and open-access code," vol. 9, 2021.

[14] URL:https://docs.vicon.com/display/Nexus212/Full+body+modeling+with+Plug-in+Gait.

[15] URL: https://www.vicon.com/hardware/cameras/vero/.

[16] URL: https://www.qualisys.com/accessories/markers/.

[17] URL: https://sites.tufts.edu/bray/tracker-motion-capture-lab-instruction/.

[18] URL: https://www.bertec.com/products/force-plates.

[19] Paillard T, Noé F, "Does monopedal postural balance differ between the dominant leg and the non-dominant leg? A review," *Human Movement Science,* vol. 74, no. 102686, 2020.

[20] Schimmel J, Groen B, Weerdesteyn V, de Kleuver M, "Adolescent idiopathic scoliosis and spinal fusion do not substantially impact on postural balance," *Scoliosis,* p. 10:18, 2015.

[21] Chiari L, Rocchi L, Cappello A, “Stabilometric parameters are affected by anthropometry and foot placement,” *Clinical Biomechanics,* vol. 17, pp. 666-677, 2002.

[22] Sozzi S, Nardone A and Schieppati M, “Specific Posture-Stabilising Effects of Vision and Touch Are Revealed by Distinct Changes of Body Oscillation Frequencies,” *Frontiers in Neurology,* vol. 12, no. 756984, 2021.

Acknowledgements

I would like to express my deepest gratitude to my supervisor Maria Rubega and my co-supervisors Paola Contessa and Erika Venturini for giving me the opportunity to carry out this thesis experience at Laboratory of Bioengineering and Movement Clinic of Azienda Ospedale-Università Padova. All the advice I was given was invaluable.